A SENSE OF SCALE: MAPPING EXOTIC ANNUAL GRASSES WITH SATELLITE IMAGERY ACROSS A LANDSCAPE AND QUANTIFYING THEIR BIOMASS AT A PLOT LEVEL WITH STRUCTURE-FROM-MOTION IN A SEMI-ARID ECOSYSTEM

by

Monica Vermillion

A thesis

submitted in partial fulfillment

of the requirements for the degree of

Master of Science in Geophysics

Boise State University

August 2020

BOISE STATE UNIVERSITY GRADUATE COLLEGE

DEFENSE COMMITTEE AND FINAL READING APPROVALS

of the thesis submitted by

Monica Vermillion

Thesis Title: A Sense of Scale: Mapping Exotic Annual Grasses with Satellite Imagery Across a Landscape and Quantifying Their Biomass at a Plot Level with Structure-from-Motion in a Semi-Arid Ecosystem

Date of Final Oral Examination: 17 July 2020

The following individuals read and discussed the thesis submitted by student Monica Vermillion, and they evaluated their presentation and response to questions during the final oral examination. They found that the student passed the final oral examination.

Nancy F. Glenn, Ph.D.	Chair, Supervisory Committee
T. Trevor Caughlin, Ph.D.	Member, Supervisory Committee
Dylan Mikesell, Ph.D.	Member, Supervisory Committee

The final reading approval of the thesis was granted by Nancy F. Glenn, Ph.D., Chair of the Supervisory Committee. The thesis was approved by the Graduate College.

DEDICATION

To the sagebrush whom were excellent teachers in both science and self – keep fighting those exotic annual grasses!

ACKNOWLEDGMENTS

First and foremost, I want to thank my friends and family for their support and constant encouragement. To my advisor Dr. Nancy Glenn, thank you for being a wonderful mentor and teacher. To my committee members Dylan and Trevor for answering countless questions. I would like to thank my funding sources Mountain Home Air Force Base (Cooperative Agreement Number: W9128F-17-2-0025) and the USDA NIFA Project Fine Fuels Management to Improve Wyoming Big Sagebrush Plant Communities Using Dormant Season Grazing (Award #2019-68008-29914). Special thank you to Sergio Arispe and April Hulet and their field crews including William Price for welcoming me onto the Fine Fuels project and introducing me to rangeland ecology. Of course, thank you to Boise Center for Aerospace Lab (BCAL) lab members present and past.

ABSTRACT

The native vegetation communities in the sagebrush steppe, a semi-arid ecosystem type, are under threat from exotic annual grasses. Exotic annual grasses increase fire severity and frequency, decrease biodiversity, and reduce soil carbon storage amongst other ecosystem services. The invasion of exotic annual grasses is causing detrimental impacts to land use by eliminating forage for livestock and creating a huge economic cost from fire control and post-fire restoration. To combat invasion, land managers need to know what exotic annual grasses are present, where they are invading, and estimates of their biomass. Mapping exotic annual grasses is challenging because many areas in the sagebrush steppe are difficult to access; yet field measurements are the main method to identify and quantify their existence. In this study, we address this challenge by exploring the use of both landscape-scale and plot-scale observations with remote sensing. First, we use satellite imagery to map where exotic annual grasses are invading and identify the native species which are being encroached upon. Second, we investigate the use of fine-scale imagery for non-destructive measurements of biomass of exotic annual grasses.

Understanding the location of exotic annual grasses is important for restoration efforts, e.g. large swath (~100m) herbicide spraying. Restoration efforts are expensive and often ineffective in areas already dominated by exotic annual grasses. Early detection of exotic annual grasses in sagebrush and native grasses communities will increase the chances of effective ecosystem restoration. We used Sentinel-2 satellite imagery in

Google Earth Engine, a cloud computing platform, to train a random forest (RF) machine learning algorithm to map vegetation in ~150,000 acres in the sagebrush steppe in southeast Idaho. The result is a classification map of vegetation (overall accuracy of 72%) and a map of percent cover of annual grass ($R^2 = 0.58$). The combination of these two maps will allow land managers to target areas of restoration and make informed decisions about where to allow grazing.

In addition to knowing what exotic annual grasses exist and their percent cover, detailed information about their biomass is important for understanding fuel loads and forage quality. Structure from Motion (SfM) is a photogrammetry technique that uses digital images to develop 3-dimensional point clouds that can be transformed into volumetric measurements of biomass. The SfM technique has the potential to quantify biomass estimates across multiple plots while minimizing field work. We developed allometric equations relating SfM-derived volume (m^3) to biomass (g/m^2) for a study area in southeast Oregon. The resulting equation showed a positive relationship ($R^2 = 0.51$) between the log transformed SfM-derived volume and log transformed biomass when litter was removed. This relationship shows promise in being upscaled to larger surveys using aerial platforms. This method can reduce the need for destructively harvesting biomass, and thus allow field work to cover a greater spatial extent. Ultimately, increasing spatial coverage for biomass will improve accuracy in quantifying fuel loads and carbon storage, providing insights to how these exotic plants are altering ecosystem services.

TABLE OF CONTENTS

LIST OF TABLES

LIST OF FIGURES

LIST OF ABBREVIATIONS

DoD	Department of Defense
MHAFB	Mountain Home Air Force Base
UV-SWIR	Ultraviolet – Shortwave Infrared
NIR	Near Infrared
SWIR	Shortwave Infrared
NDVI	Normalized Difference Vegetation Index
OSAVI	Optimized Soil Adjusted Vegetation Index
SAVI	Soil-Adjusted Vegetation Index
EVI	Enhanced Vegetation Index
GEE	Google Earth Engine
RF	Random Forest
SVM	Support Vector Machines
BLM	Bureau of Land Management
SCR	Saylor Creek Range
JBR	Juniper Butte Range
OPUS	Online Positioning User Service
ARI	Anthocyanin Reflectance Index
CCCI	Canopy Chlorophyll Content Index
UAV	Unmanned Aerial Vehicles
AGB	Above Ground Biomass

PFT	Plant Functional Type
UAS	Unmanned Aerial Systems
SfM	Structure from Motion
ROI	Region of Interest
DSM	Digital Surface Model
CHM	Canopy Height Model
RMSE	Root Mean Square Error

CHAPTER ONE

Introduction

Exotic Annual Grasses in Semi-Arid Ecosystems

Drylands play a critical role as global terrestrial carbon sinks. The extent of their impact is still being quantified, Poulter et al. (2014) found in 2011 that semi-arid biomes were responsible for 60% of terrestrial carbon uptake in the Southern Hemisphere. Semi-arid ecosystems are sensitive to changes in precipitation and air temperature. Shifts in precipitation and air temperature related to climate change are expected to negatively impact semi-arid ecosystems and reduce their global carbon uptake (Ahlström et al., 2015; Smith et al., 2019). The sagebrush-steppe ecosystem, a dryland ecosystem type, covers much of the western U.S. and is a dominant ecosystem type in the Great Basin and Range (Figure 1.1). One of the largest threats to the sagebrush-steppe ecosystem, specifically low elevation sites, is the introduction of invasive exotic annual grasses such as cheatgrass (*Bromus tectorum*) and medusahead (*Taeniatherum caput-medusae*). Cheatgrass and other exotic annual grasses dominate native vegetation in many geographic areas of the Great Basin and Range, with profuse expansion in the Snake River Plain in southwest Idaho (Figure 1.1). A 2014 study indicates that over 85% of the vegetation cover in the Snake River Plain consists of cheatgrass (Boyte & Wylie, 2016). Flat areas of low to mid elevation sagebrush steppe like the Snake River Plain are at high risk for invasion. The invasion of these exotic annual grasses can be attributed to

disturbances such as fire, urbanization, land use, and improperly managed grazing regimens (Chambers et al., 2014; DiTomaso et al., 2010).

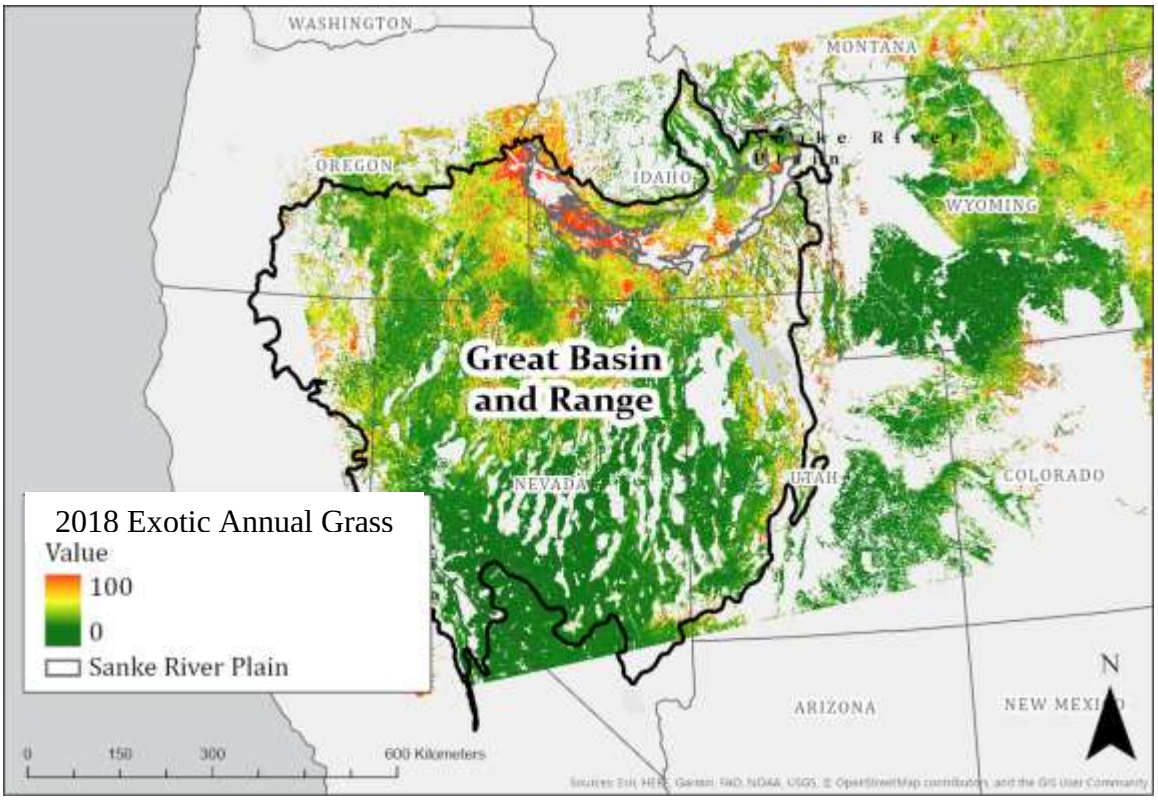

Figure 1.1 Exotic annual grass percent cover of the Great Basin. The Snake River Plain has high percent cover (modified from Boyte et al., 2018).

The introduction of exotic annual grasses has led to a decrease in biodiversity, alteration of the natural fire cycle, and changes in ecosystem services that the sagebrush steppe provides. An undisturbed, healthy sagebrush steppe ecosystem can be described as heterogenous and diverse, with a large amount of biological soil crust in the interspace of native shrubs, forbs, and perennial bunchgrasses (Chambers et al., 2014). Native plant communities grow slowly to establish a deep root system making them resilient to the natural water scarcity. In contrast, cheatgrass and medusahead have shallow roots that allow for rapid soil moisture uptake following precipitation events and quickly thrive by using up ecosystem nutrients (namely Nitrogen) (Boyte et al., 2015). These traits allow

them to easily outcompete native plants, altering the landscape to a dense homogenous cover of exotic annual grasses, and reducing the biodiversity.

The positive feedback loop between invasive grasses and fire in the Great Basin is well documented (shown in Figure 1.2). The presence of cheatgrass has increased the frequency of burning from a 50-100-year cycle to a mere 5-10-year cycle (Moriarty et al., 2015). The increase in atmospheric CO_2 has promoted cheatgrass productivity, resulting in greater biomass, creating an increase in fuel load and fire severity (Ziska et al., 2005). These alterations of the fire cycle have widespread ecological impacts and decrease the resistance of native plant communities to invasive species (Chambers et al., 2014; Peeler & Smithwick, 2018). Condon et al. (2018) quantified site resistance to biotic factors directly altered by fire and grazing. The decrease in resistance and increased fire cycle makes previously burned areas especially vulnerable to invasion from exotic annual grasses. Cheatgrass presence was found in 47% of areas that have previously burned in the Great Basin, increasing the probability those areas will burn again (Bradley et al., 2018).

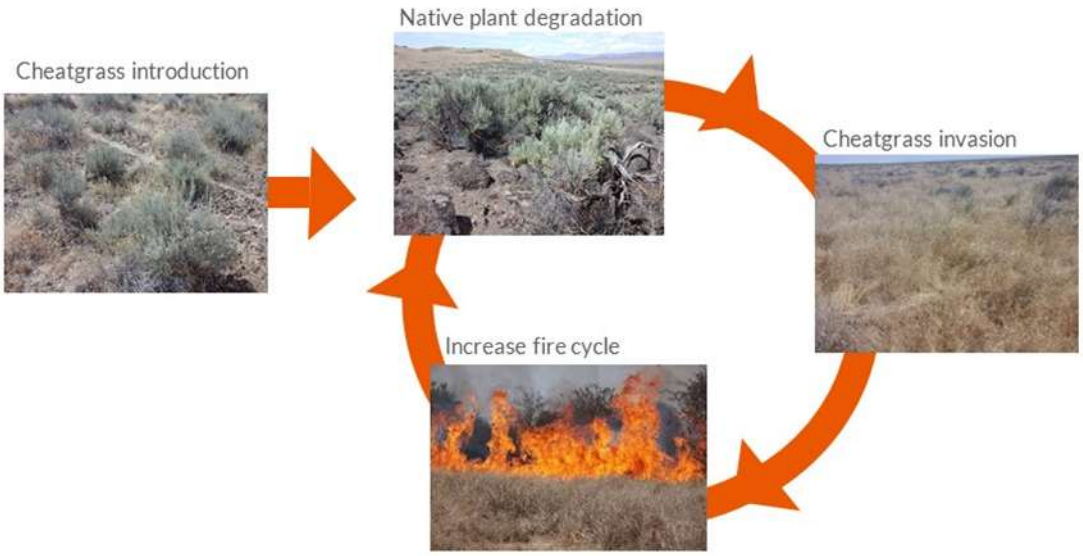

Figure 1.2 Positive feedback loop where the altered fire cycle includes cheatgrass invasion which promotes fire and leaves native areas susceptible to further invasion.

Bradley et al. (2006) suggested the shift from native shrubs and bunchgrasses to invasive annual grasses has resulted in a loss of carbon storage upwards of 8 ± 3TgC and could lead to another 50±20 TgC in the future.

Remotely Sensed Data for Management of Exotic Annual Grasses

The extensive spread of exotic annual grasses is difficult for land managers to control. Current land management strategies for cheatgrass and other exotic annual grasses focus on control (e.g. spraying herbicides) and restoration of plant ecosystems that are not as susceptible to invasive species, including planting non-natives (DiTomaso et al., 2010). Knowing the location of large swaths of exotic annual grasses on a landscape scale can help land managers plan for treatments. Identifying undisturbed native shrub communities can help identify areas to protect from future disturbances and focus post-fire restoration efforts. Davies et al. (2011) in describing conservation strategies for the sagebrush steppe ecosystem called for more research on identifying areas for restoration, and a need to reduce disturbances, such as human-caused fires, to

prevent the spread of exotic annual grasses. Remote sensing offers a solution to better understand the status of and focus conservation efforts of the sagebrush steppe by offering higher spatial and temporal data than field collection alone. Remote sensing of drylands has dramatically improved through innovative combinations of remotely sensed data, improvements of algorithms specifically for dryland ecosystems and improvements on how *in situ* data are collected when used with remotely sensed data (Smith et al., 2019).

My thesis focuses on developing and applying two different optical remote sensing processes at fine (cm) to medium (m) spatial scales to better understand the impacts of exotic annual grasses and to help inform land managers. The second chapter uses satellite imagery to identify areas for restoration and conservation by mapping vegetation at a landscape scale. The third chapter works to develop a relationship between volume and biomass of exotic annual grasses using Structure-from-Motion point cloud data at a plot scale. Deriving biomass from remotely sensed data can provide researchers and land managers better insight to the impacts of exotic grasses on ecosystem structure and function.

CHAPTER TWO: MAPPING DOMINANT VEGETATION AND CHEATGRASS COVER IN THE SNAKE RIVER PLAIN USING SENTINEL-2 AND RANDOM FOREST MACHINE LEARNING IN GOOGLE EARTH ENGINE

Introduction

Importance of Mapping the Sagebrush Steppe Ecosystem for Science and Land Management

Understanding the distribution of vegetation at a medium spatial scale (10s of m) over a large geographic area is critical for land managers to understand ecosystem health and to plan for restoration. To better inform ecosystem health of the sagebrush steppe, it is critical to know where exotic annual grasses, such as cheatgrass are invading. The pre-disturbance vegetation composition of a landscape is a major predictor of post-disturbance recovery (Jones et al., 2018). Annual vegetation maps can be used to assess the impact of disturbance and determine the effectiveness of restoration efforts by land managers such as the U.S. Department of Defense (DoD). In order to assess these impacts, accurate maps of the distribution and density of both invasive and native plants are necessary.

The DoD is the third largest land manager nationwide, including management of large tracts of land in the Snake River Plain as part of the Mountain Home Air Force Base (MHAFB) installations. Human disturbance and human-caused fires from activities such as ground training and artillery exercises on these installations cause stress to the native ecosystem, resulting in invasive species spread. Subsequently, the increase in fire

risk from cheatgrass can drastically impact training schedules, routines, and economic costs to the DoD. The DoD needs regularly updated vegetation maps to gauge how disturbances impact the vegetation on the managed land. Annual vegetation maps are critical to understanding how exotic annual grasses have spread, to gauge effectiveness of restoration techniques, and to determine areas to be protected. Since installations are typically extensive, located in remote areas with few access roads, and there is danger in performing field work due to unexploded ordinances, it is challenging to understand the composition of the plant communities. Additionally, creating annual vegetation maps can be time and labor intensive, and often expensive. Advances in remote sensing technology, such as high-resolution satellite imagery, and advances in computing offer a potential solution to mapping vegetation at a species level on DoD installations.

Optical Remote Sensing of Semi-Arid Ecosystems

Sentinel-2 satellite imagery provides regular observations of the entire spatial extent of MHAFB. Sentinel-2 is an optical satellite launched by the European Space Agency in 2015 and was chosen for this study because of the high temporal resolution (every 5 days at the equator, more frequently in higher latitudes) and the medium spatial resolution of 10 – 20m pixels (Table 2.1). The imagery is multispectral with 13 spectral bands ranging from the ultraviolet to the shortwave infrared (UV-SWIR) (Drusch et al., 2012). Sentinel-2 imagery have been used to map vegetation and biocrust in dryland ecosystems in Nevada through spectral unmixing of biocrust *in-situ* measurements (Panigada et al., 2019). Multiple studies have shown successful mapping of cheatgrass using optical remote sensing (Boyte et al. 2016; Bradley et al. 2018; Van Gunst et al. 2017; Peterson 2015; West et al. 2017). For example, West et al. (2017) demonstrated the

use of Landsat imagery and species-distribution models to map and model percent cheatgrass cover post-fire in the Medicine Bow National Forrest.

Table 2.1 Sentinel-2 bands, spectral wavelengths (center), and spatial resolutions, used in the study (Drusch et al., 2012). NIR is near infrared and SWIR is shortwave infrared.

Sentinel-2 Band	Center Wavelength (µm)	Resolution (m)
Band 2 - Blue	0.490	10
Band 3 - Green	0.560	10
Band 4 - Red	0.665	10
Band 5 - Vegetation Red Edge	0.705	20
Band 6 - Vegetation Red Edge	0.740	20
Band 7 - Vegetation Red Edge	0.783	20
Band 8 - NIR	0.842	10
Band 8a – Narrow NIR	0.865	20
Band 11 - SWIR	1.610	20
Band 12 - SWIR	2.190	20

The 5-day repeat cycle of Sentinel-2 is ideal for capturing the phenology of vegetation in the sagebrush steppe. Phenology can be described as the life cycle of plants, and is used to track their growth, major biological events and photosynthesis. In the Great Basin and Range, cheatgrass phenology has been studied using Landsat-derived Normalized Difference Vegetation Index (NDVI) spectral indices to better understand the relationship of cheatgrass and precipitation events (Clinton et al., 2010). Cheatgrass and other invasive annuals can be distinguished based on their early-season phenology, described as a sharp green-up period followed by a rapid decrease in growth and production to early

senescence. Spectral indices are standard metrics of phenological responses of ecosystems in remote sensing.

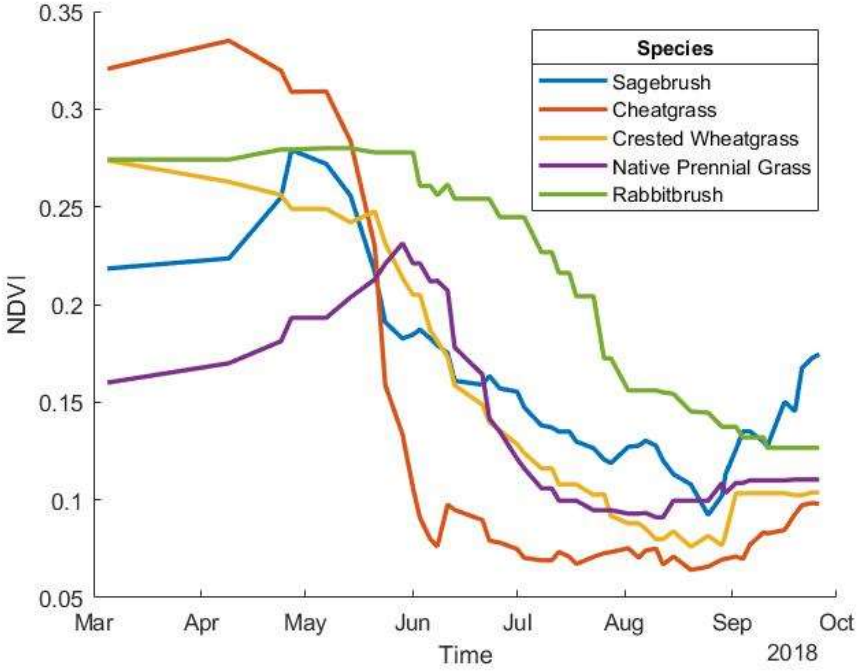

Figure 2.1 Temporal differences in NDVI of select species from the sagebrush steppe ecosystem in this study, derived from 2018 Sentinel-2 data.

A major challenge in optical remote sensing of semi-arid ecosystems is the heterogeneity of the landscape and sparse vegetation cover. The latter results in the spectral response signal being mixed with the high reflectance of the bare ground. This makes it difficult to de-couple the vegetation from the ground reflectance (Smith et al., 2019). To address these challenges two approaches are often used in remote sensing: spectral indices developed for semi-arid ecosystems and "big data". In addition to NDVI, multiple spectral indices have been successful in dryland ecosystems such as Optimized Soil Adjusted Vegetation Index (OSAVI), Soil-Adjusted Vegetation Index (SAVI), and the Enhanced Vegetation Index (EVI). For a comprehensive review of spectral indices for drylands, refer to West et al. (2017). The use of a phenological time-series of Sentinel-2

images proved to effectively map invasive pines (*Pinus radiata*) in Chile (Forster et al., 2017). This study also found that increasing the number of Sentinel-2 images had the greatest impact on increasing the accuracy. Many studies have shown successful mapping of cheatgrass using a phenological time-series approach with satellite data (Clinton et al., 2010; Peterson, 2015; West et al., 2017). Remote sensing platforms have been used to study dryland ecosystems since the 1980's; however recent advances in cloud computing, open source technology, and instrumentation/satellites have led to a better understanding of ecosystem dynamics in drylands.

Google Earth Engine for Classification

Traditionally, supervised classifications have been incredibly time intensive in part because processing of satellite data required manually downloading data from the data source, sifting through dates with cloud-free images, and classification of every image. Google Earth Engine (GEE) is a cloud computing interface specifically designed for scientific research in the remote sensing community. The GEE platform eliminates the need for local data acquisition and data processing on all imagery, and processing can be reduced to a few lines of code in the user's browser (Gorelick et al., 2017; Kumar et al., 2018).

Machine-learning techniques within GEE can be leveraged to improve the accuracy of species classification by finding trends in remotely sensed data (Gallagher, 2018). Random forest (RF) is an ensemble machine learning algorithm that can be used to take training data and create either a classification or regression model (Belgiu & Drăgu, 2016; Pavlov, 2019). It is iterative in design to address over-fitting and instability that can arise when using conventional classification tree-based approaches. RF has been

shown to outperform Support Vector Machines (SVM), another machine learning algorithm, in land cover classification using a two year time-series of Landsat data in France with an overall accuracy of 83% using RF compared to 77% for SVM (Pelletier et al., 2016). The workflow of GEE and RF are reproducible and thus we eliminate the need to manually reprocess satellite data when updated field and satellite imagery become available. In other words, the workflow allows us to support monitoring for a restoration program. GEE and RF regressions have been used to map historical percent cover maps of four plant functional types across the Great Basin and Range at a 30m resolution, but relies on spatially sparse training data (Jones et al., 2018). We leverage these advances in satellite technology, cloud computing, and machine learning to develop accurate maps of semi-arid ecosystems at a medium spatial scale.

Research Questions

1. How effectively can random forest (RF) map vegetation at a landscape-scale using time-series of Sentinel-2 imagery over a semi-arid ecosystem to support land management?
2. How can cloud computing be leveraged to develop a reproduceable workflow for the purpose of vegetation monitoring in the sagebrush steppe?

Methods

Study Area: Mountain Home Air Force Base

In southwest Idaho, the DoD is responsible for managing ~150,000 acres of sagebrush steppe ecosystem, primarily as part of the MHAFB. The MHAFB installations cover an elevation gradient from 800 to 1667 m (Figure 4). The relatively flat topography, low elevation, and extensive fire history make MHAFB installations prone to

cheatgrass invasion. Boyte et al. (2016) found cheatgrass does not currently grow at elevations above 2000 m, therefore the entire study area is at risk of invasion and that invasion will likely lead to a high percent cheatgrass cover. The installations are surrounded by Bureau of Land Management (BLM) land, private agriculture, and state parks. There is intense land use both from training and grazing allowed on these installations. Subsequently, large parts of the installations are dominated with invasive annual plants, specifically cheatgrass, which have increased the cost of fire management

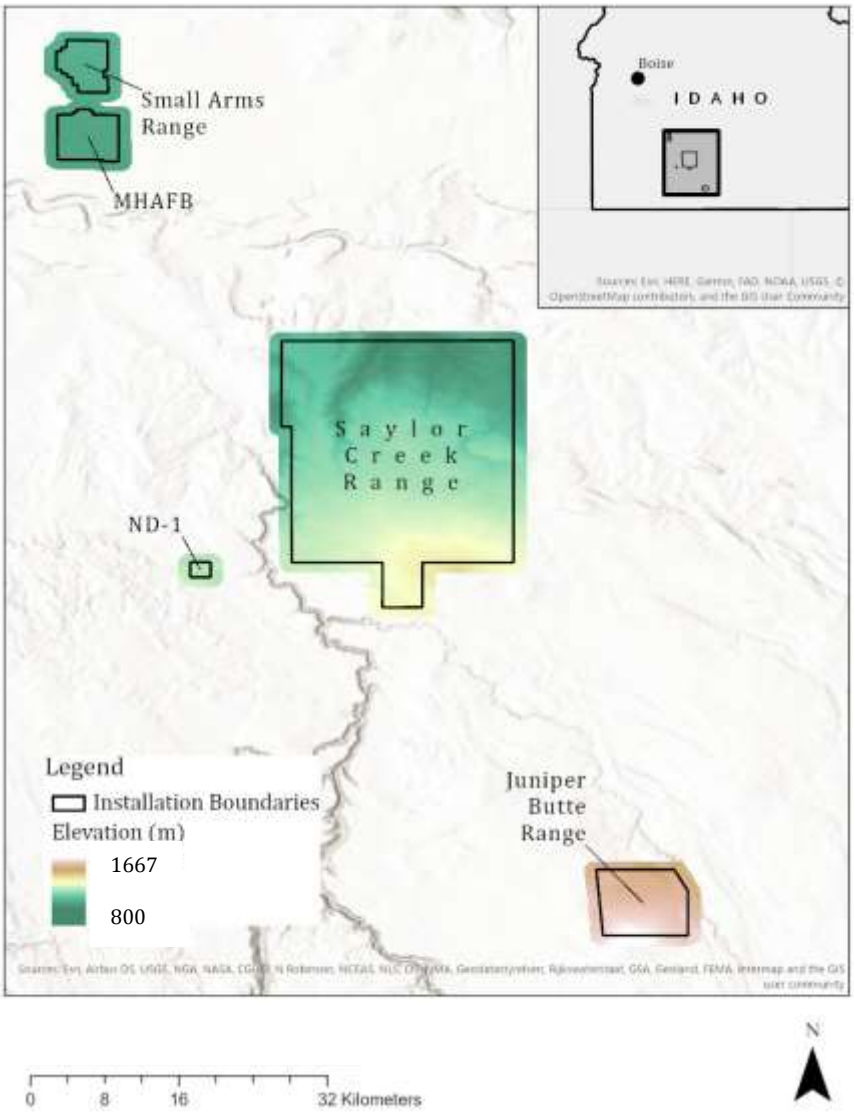

Figure 2.2 Extent and elevation of MHAFB installations.

and training time. For example, in 2011, frequent fires removed significant amounts of vegetation, causing major dust storms that shut down training for multiple weeks.

The diversity of the landscape both in vegetation composition and land management makes MHAFB an ideal study area for mapping representative low elevation sagebrush ecosystems. The ecosystem ranges from highly degraded areas of cheatgrass to pristine low elevation sagebrush steppe, as well as areas of restoration where non-native perennial grasses were planted. One installation, Saylor Creek Range (SCR), is highly disturbed from bombing and is dominated with cheatgrass, whereas Juniper Butte Range (JBR) has few disturbances and therefore is dominated with native shrubs. A major challenge MHAFB land managers face is identifying target areas for restoration. Remote sensing techniques and advances in technology provide a potential method to map the entire ~150,000 acres at a species level.

Field Plot Design and Protocol

Field data were collected with the purpose of being used as training data for a remote sensing land cover classification map. Field data collection took place from June-July 2018, a time period that is ideal for distinguishing plant species in the study area. The field protocol was designed to capture the diversity of vegetation species and their spatial distributions, to be scalable to Sentinel-2 satellite imagery, and to be collected during a single field season. Locations of field plots were chosen at random locations (given road access) and with a minimum of 30 training plots for each plant functional type, the actual number of plots collected for each target species type is shown in Table 2.2.

Table 2.2 Field data collection including species, number of plots, and percent cover.

Species Common Name	Scientific Name**	Target Number of Plots	Min. cover (%)	Plots Collected
Wyoming Big and Mountain Big Sagebrush	*Artemisia tridentata*	30	15	35
Green and Grey Rabbitbrush	*Chrysothamnus*	30	10	38
Winterfat*	*Krascheninnikovia lanata*	30*	15	13
Shadscale*	*Atriplex confertifolia*	30*	10	2
Forage Kochia*	*Bassia prostrata*	30*	10	23
Cheatgrass	*Bromus tectorum*	30	30	39
Sandberg Bluegrass	*Poa secunda*	30*	30	7
Crested Wheatgrass	*Agropyron cristatum*	30	15	39
Exotic Annuals: Burbuttercup, Clasping pepperweed, Russian thistle	*Ceratocephala testiculata, Lepidium perfoliatum, Kali tragus*	30	10	11
Playa		10	70	10
Data added using GEE				
Bare Ground or Impervious				42
Cultivated or Riparian				22

**if possible ** scientific names from USDA*

Each field plot represents a 20 x 20 m area and consisted of 5 RTK (Real Time Kinematic) GPS points taken 2 m above ground at the central point of the field plot and 10 m in the four cardinal directions (Figure 2.3a). The protocol was informed and modified based on a 2016 data collection of the same study area (Enterkine, 2019). The 20 x 20 m plot was chosen to correspond to roughly 2 x 2 pixels in the Sentinel-2 multispectral imagery for bands 2-8, 11, and 12 (Table 2.1). This field plot design accommodated registration mismatch within Sentinel-2 specifications and mitigates the

influence of neighboring areas on the signal of observed pixels. At each of the 5 GPS points a nadir (vertically downward facing) image was taken with a 16-megapixel all-weather Nikon Coolpix AW110 camera mounted on a 1 m boom attached perpendicularly to a 2 m pole (Figure 2.3b). Each image covered approximately 2.8 m x 2.1 m area.

A minimum percent cover, estimated ocularly, was established for each species to be considered as a training plot for that species (Table 2.2). These minimum thresholds were set based on previous field experience in this and other low-elevation sagebrush steppe ecosystems (e.g. Enterkine, 2019; Spaete et al., 2016). The plots were collected to have a representative distribution of percent cover and composition for the dominant species in the study area, e.g. a sagebrush plot with a biocrust understory and sagebrush plots with invasive grass understory.

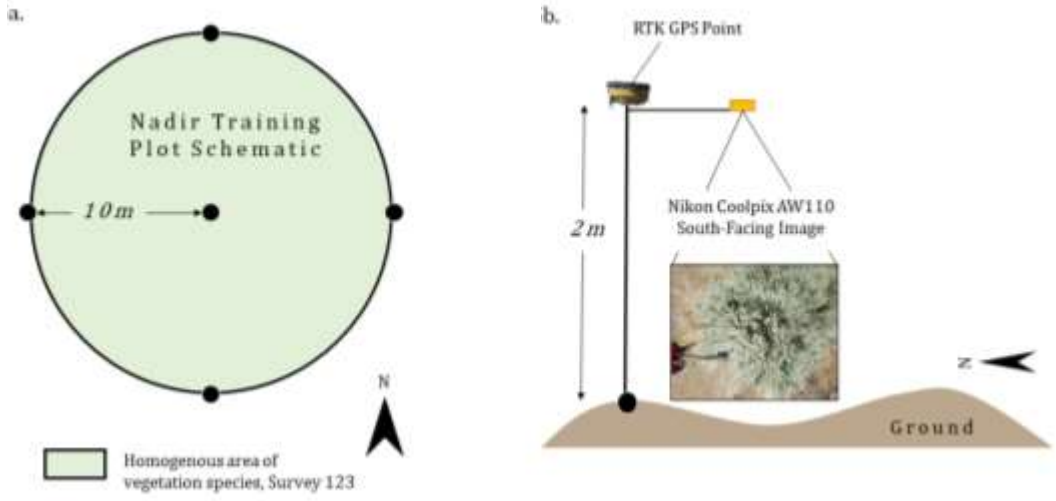

Figure 2.3 Field plot schematic from a birds-eye view, one Survey 123 survey was taken per plot (a); data collected 10 m in each cardinal direction from the center of the field plot included an RTK GPS point and Nikon Photo (b).

At each field plot, we recorded all species found in the plot, the dominant species, and additional field notes using a tablet running the ESRI Survey123 app (see Appendix A). Field plots were randomly stratified across the MHAFB installations to capture the variability of the targeted vegetation types. A total of 256 field plots were collected.

Processing Field Data

To quantitatively determine the vegetation cover for each field plot, SamplePoint software (version 1.59, a free image analysis software developed for the United States Department of Agricultural Research Service; samplepoint.org) was used on the nadir images as a time-efficient alternative to the traditional field-based point-frame technique. This method lends itself to remote sensing because most of the signal from the satellites is attributed to canopy cover not the understory of the vegetation. In SamplePoint, a grid was overlaid on each image, and research assistants (in the lab) classified the vegetation species at each crosshair of the grid. Fractional cover of each plot was calculated by taking mean cover type from the five images associated with each plot. Dominate species were aggregated in some cases with the purposes of creating training classes of sufficient size for modeling (Table 2.3).

Table 2.3 Aggregated vegetation classes for the purposes of training.

Aggregated Class	Species in Class	
	Common Name	Scientific Name
Sagebrush	Sagebrush	*Artemisia tridentata*
Bare	Dirt without vegetation or biocrust present	
Bluebunch Wheatgrass	Bluebunch Wheatgrass	*Pseudoroegneria spicata*
Cheatgrass	Cheatgrass	*Bromus tectorum*
Crested Wheatgrass	Crested Wheatgrass	*Agropyron cristatum*
Exans	Russian Thistle, Bur Buttercup, Clasping Pepperweed	*Salsola tragus, Ceratocephala testiculata, Lepidium perfoliatum*
Forage Kochia	Forage Kochia	*Bassia prostrata*
Native Grasses	Thurber's Needlegrass, Indian Ricegrass	*Achnatherum thurberianum, Achnatherum hymenoides*
Mustard	Tumble Mustard	*Sisymbrium altissimum*
Sandberg bluegrass	Sandberg bluegrass	*Poa secunda*
Rabbitbrush	Green Rabbitbrush, Grey Rabbitbrush	*Chrysothamnus viscidiflorus, Ericameria nauseosa*
Winterfat	Winterfat	*Krascheninnikovia lanata*
Playa		

An RTK GPS base station collected data in the field for more than 2 hours, and base station data were uploaded to Online Positioning User Service (OPUS) Solutions static processing (2 weeks after data collection per recommendation by OPUS). The output from OPUS Solutions was used to correct the raw RTK GPS points for field plots in MagnetTools Software. Base stations were set as control points and corrected to the output location based on OPUS solutions. This shifted the corresponding RTK points on the sub-cm scale which is an order of magnitude smaller than the scale of the field plots

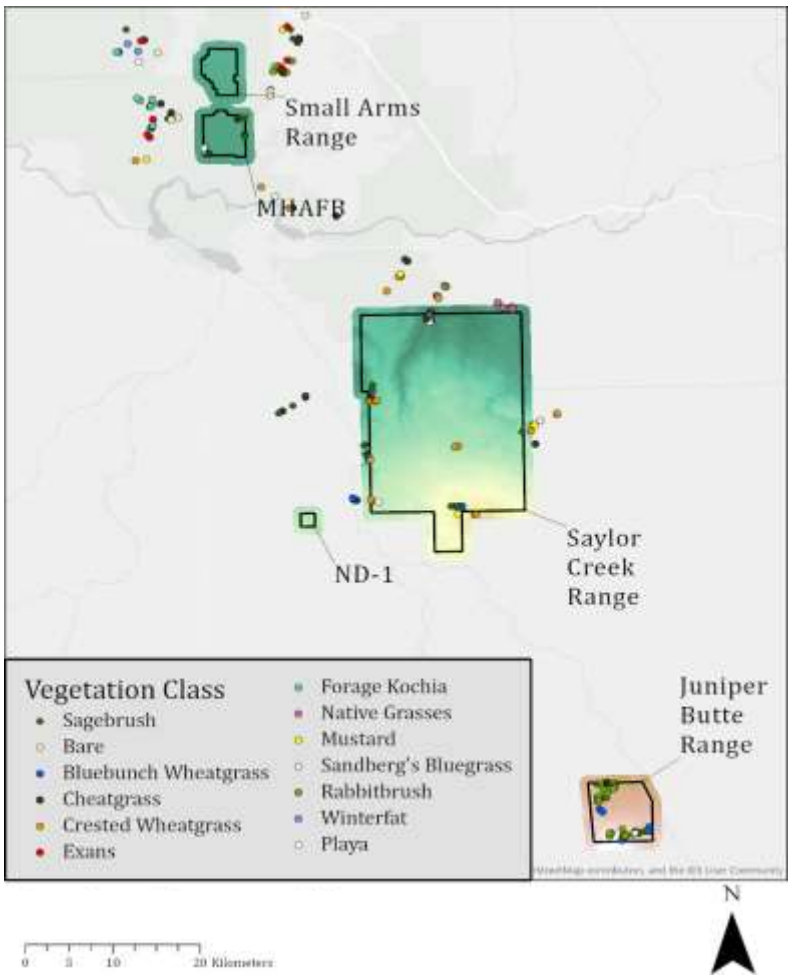

Figure 2.4 Extent and elevation of Mountain Home Air Force Base installations.

and satellite data. The center points of each plot were buffered by 10 m to create a circular polygon to be associated with fractional percent cover obtained from the SamplePoint data. The fractional cover provides a quantitative metric for determining the expected dominant spectral signal in the plot. We found that bare ground was the dominant (highest percent cover) cover type for many plots, even though the plot was initially collected as a sagebrush plot. To address this, plots with bare cover greater than 70% were considered bare dominant. In these plots, we then identified the second highest percent cover and if that met the minimum percent cover for the species, then the plot

was classified as that of the second highest percent cover. For example, a sagebrush plot with 40% bare ground and 30% sagebrush would be classified at sagebrush. If the highest cover species and second highest cover species are within 5% cover of each other, the plot is considered mixed and discarded for training. Field plots were given a single classification of their dominant species cover, e.g. sagebrush, to be used in the classification (Figure 2.4). Ancillary data for additional land cover types not surveyed (e.g. water, pavements) were identified using high-resolution imagery (NAIP, Worldview via Google Earth in GEE). Additionally, several areas of playa and bare ground were delineated in the field using the RTK GPS. After accounting for bare ground dominated plots and mixed pixels, there were 252 plots used in the classification, maintaining a range of species and percent cover (Figure 2.5). For the regression analysis of cheatgrass distribution, the percent cover of cheatgrass was taken from each point to be used in the regression. The shapefile (Figure 2.4) with the vegetation class and percent cheatgrass cover were uploaded as an asset into GEE.

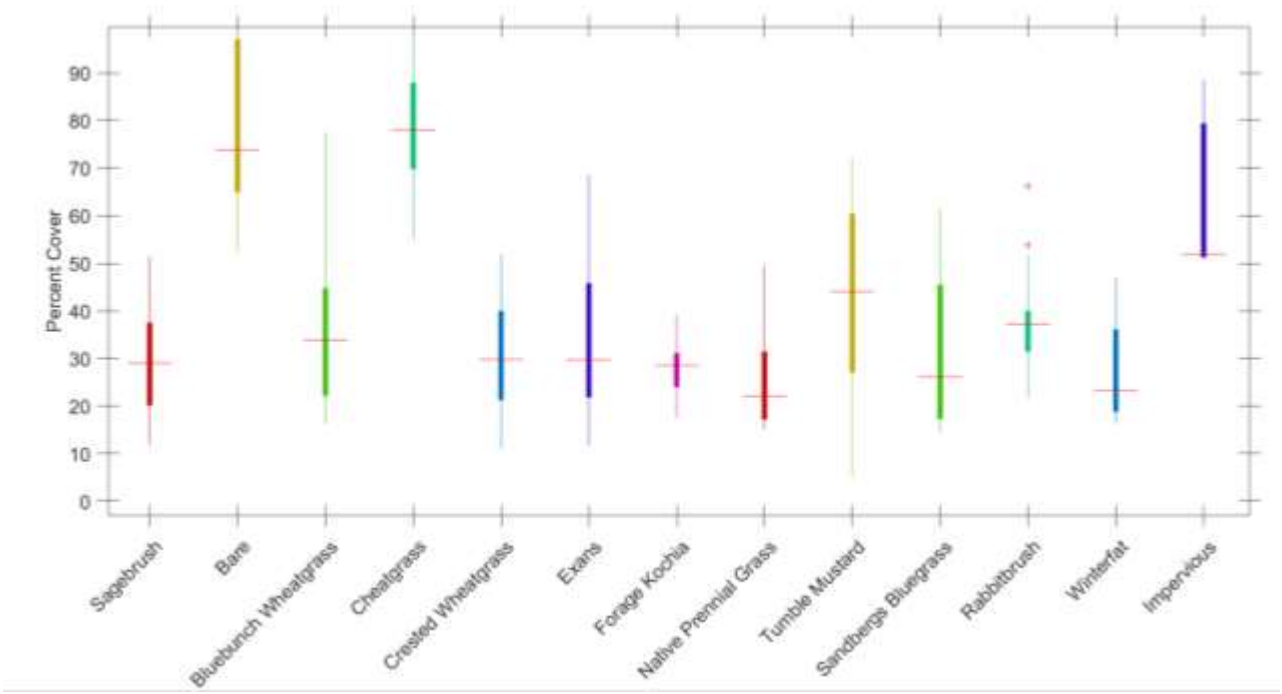

Figure 2.5 Boxplot showing distribution of percent cover for dominant vegetation classes.

Sentinel-2 Preprocessing

We aggregated Sentinel-2 Level 1 (L1) top of atmosphere data in GEE from August 2017-August 2018. On August 25, 2018, a fire occurred within the study area which influenced the spectral signal of some of the training plots captured by Sentinel 2. While some Sentinel-2 L2 data are available on GEE, the data do not fully cover the study area and therefore L1 data were used. The data were filtered to remove images with greater than 5% cloud cover. In addition, the GEE cloud mask for Sentinel-2 was applied to the data. The study area covers 3 tiles of Sentinel-2 imagery data, where one tile is offset, and imagery is acquired during a different overpass time. To address the offset in imagery, weekly mosaics were created from the 3 tiles. This removed the temporal offset and ensured the same number of images for each plot.

RF Classification and Regression in GEE

From the time series of Sentinel-2 data we computed the spectral indices listed in Table 2.4 for every weekly mosaic. The buffered shapefile of the field plots was imported to GEE and overlaid on the imagery. For each field plot, the mean reflectance for each band along with the vegetation indices (from Table 2.4) for every image in the stack were calculated. These data were then used as the predictor variables in training the RF decision tree. Each field plot has 102 predictor variables associated with it. For both the classification and regression analysis, 70% of field plots were used for training and 30% were used for validation.

Table 2.4 Computed spectral indices used in the random forest models.

Index or Ratio	Abbreviation	Formula	Reference
Anthocyanin Reflectance Index	ARI	$\left(\frac{1}{Green_{560nm}}\right) - \left(\frac{1}{RedEdge_{704nm}}\right)$	(Gitelson et al., 2001)
Canopy Chlorophyll Content Index	CCCI	$\frac{\frac{NIR_{864nm} - RedEdge_{780nm}}{NIR_{864nm} + RedEdge_{780nm}}}{\frac{NIR_{864nm} - Red_{665nm}}{NIR_{864nm} + Red_{665nm}}}$	(Fitzgerald et al., 2010)
Enhanced Vegetation Index	EVI	$\left(\frac{2.5 * (NIR_{833nm} - Red_{665nm})}{NIR_{833nm} + (6 * Red_{665nm}) - (7.5 * Blue_{492nm}) + 1}\right)$	(Gurung et al., 2009)
Normalized Difference Vegetation Index	NDVI	$\frac{NIR_{833nm} - Red_{665nm}}{NIR_{833nm} + Red_{665nm}}$	(Rouse et al., 1973)
Near InfraRed-Normalized NDVI	NDVIxNIR	$\frac{(NIR_{833nm} - Red_{665nm})}{(NIR_{833nm} + Red_{665nm})} * NIR_{833nm}$	*
Normalized Difference SWIR-Green	ND_B11B3	$\frac{SWIR_{1612nm} - Green_{560nm}}{SWIR_{1612nm} + Green_{560nm}}$	*
Normalized Difference Narrow NIR-Red	ND_B8AB4	$\frac{NIR_{864nm} - Red_{665nm}}{NIR_{864nm} + Red_{665nm}}$	*
Normalized Difference Narrow NIR-RedEdge	ND_B8AB5	$\frac{NIR_{864nm} - RedEdge_{704nm}}{NIR_{864nm} + RedEdge_{704nm}}$	*

**Modified NDVI utilizing spectral bands unique to Sentinel-2*

For the classification map, the discretized dominant species assigned to each plot was the response variable. The RF decision tree was then trained with 70% of the plots using the spectral data for 2018 described above. The trained classifier was applied to the entire study area to determine the classification of every pixel (Figure 2.6a). A nearest neighbor resampling was applied to the final classification to smooth the map for aesthetics, and to remove a speckling effect. This did not change the confusion matrix.

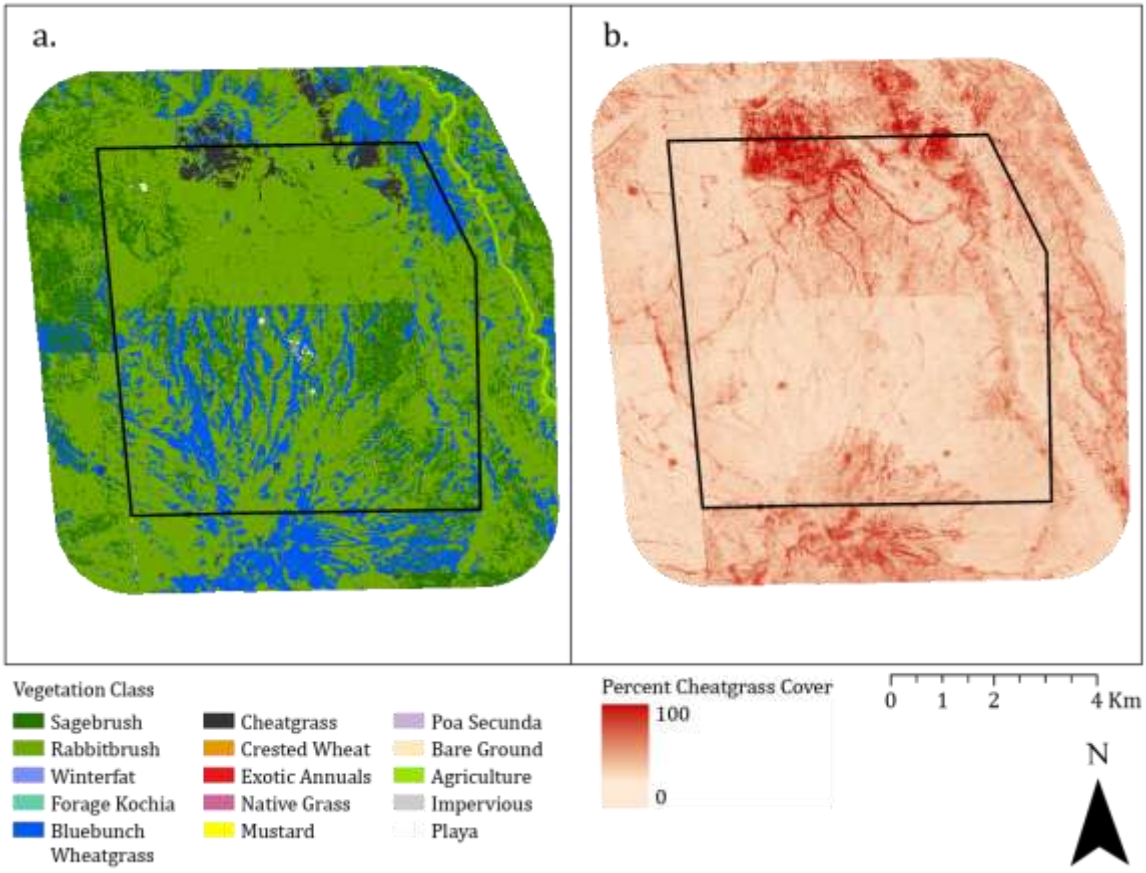

Figure 2.6 Vegetation classification map of Juniper Butte Range installation (a); and corresponding percent cheatgrass cover map from regression (b)

The regression analysis uses the percent cover of cheatgrass associated with each field plot as the response variable and the same spectral data used in the classification as the predictor variables. Again, the RF decision tree classifier was trained, but this time in

regression mode to determine percent cover as a continuous variable, compared to the discrete classification. The trained model was then run over the entire study area. The resulting map gives every pixel a percent cover of cheatgrass (Figure 2.6b).

Results

The confusion matrix (Table 2.5) details the quantitative results from the classification for each species type for all MHAFB installations. The overall accuracy of the classification was 72.0%. The producer's accuracy was 66.3%, and the user's accuracy was 62.2%. The lowest accuracies occur in classes where there were less than 10 training plots. The lack of training data for a vegetation class is attributed to the lack of vegetation present in the study area. Sandberg's bluegrass was not highly abundant, and few patches were found on the installations resulting in limited training (n=7) and test (n=1) data. In many cases, Sandberg's bluegrass was mixed with cheatgrass or crested wheatgrass and not the dominant species. Winterfat had a low user's accuracy (25%) due to confusion with bare ground. Further inspection of the winterfat field plots indicate they are dominated by bare ground cover and are near a dirt road. As expected in this heterogeneous ecosystem, misclassifications can be attributed to spectral mixing and a low vegetation signal. Sagebrush had a high producer's accuracy (60.5%) and in the few instances of misclassification, sagebrush was confused with native bunchgrasses, which are often the understory of sagebrush. Rabbitbrush is only confused with sagebrush, in part due to their similar phenological signals, and in part due to the training plots collected at Juniper Butte Range where rabbitbrush was often co-dominant with sagebrush, resulting in a mixed signal in the training data. Bluebunch wheatgrass has a

high producer's accuracy at 91.7%, however it has a low user's accuracy of 47.8% due to the confusion of sagebrush plots as bluebunch wheatgrass.

Table 2.5 Confusion matrix for the vegetation classification map of all MHAFB installations.

Confusion Matrix			Predicted															
			Sagebrush	Bare	BBWG	Cheatgrass	CW	Exan	Forage Kochia	Native Grass	Mustard	Sandberg's Bluegrass	Rabbitbrush	Winterfat	Agriculture	Impervious	Playa	User's Accuracy
Actual	Total:	257	43	22	12	24	27	9	15	12	3	1	40	2	21	18	8	62.2%
	Sagebrush	35	26	1	0	0	2	0	1	0	0	0	5	0	0	0	0	74.3%
	Bare	23	0	15	0	1	0	1	2	3	0	0	0	0	0	1	0	65.2%
	Bluebunch Wheatgrass	17	3	0	11	0	1	0	1	0	0	0	1	0	0	0	0	47.8%
	Cheatgrass	23	3	0	0	15	3	1	0	0	1	0	0	0	0	0	0	65.2%
	Crested Wheatgrass	22	2	0	0	0	17	0	1	1	0	1	0	0	0	0	0	77.3%
	Exan	11	0	1	0	4	0	6	0	0	0	0	0	0	0	0	0	54.5%
	Forage Kochia	9	0	0	0	0	0	0	8	0	0	0	0	1	0	0	0	88.9%
	Native Grass	12	4	1	0	0	1	0	0	6	0	0	0	0	0	0	0	50.0%
	Mustard	7	2	0	1	2	0	0	0	0	2	0	0	0	0	0	0	28.6%
	Sandberg's Bluegrass	7	0	0	0	2	3	1	0	1	0	0	0	0	0	0	0	0.0%
	Rabbitbrush	38	2	0	0	0	0	0	1	1	0	0	34	0	0	0	0	89.5%
	Winterfat	4	0	2	0	0	0	0	1	0	0	0	0	1	0	0	0	25.0%
	Agriculture	22	1	0	0	0	0	0	0	0	0	0	0	0	21	0	0	95.5%
	Impervious	19	0	2	0	0	0	0	0	0	0	0	0	0	0	16	1	84.2%
	Playa	8	0	0	0	0	0	0	0	0	0	0	0	0	0	1	7	87.5%
	Producer's Accuracy	66.3%	60.5%	68.2%	91.7%	62.5%	63.0%	66.7%	53.3%	50.0%	66.7%	0.0%	85.0%	50.0%	100.0%	88.9%	87.5%	Overall Accuracy 71.98%

Qualitatively the classification captured the species distributions of the installations. The Base and Small Arms Range (Figure 2.7) have many exotic annuals but still contain a few areas dominated by sagebrush such as the northwest corner of the Base. However, both the classification and regression maps show those areas are next to areas of high cheatgrass cover.

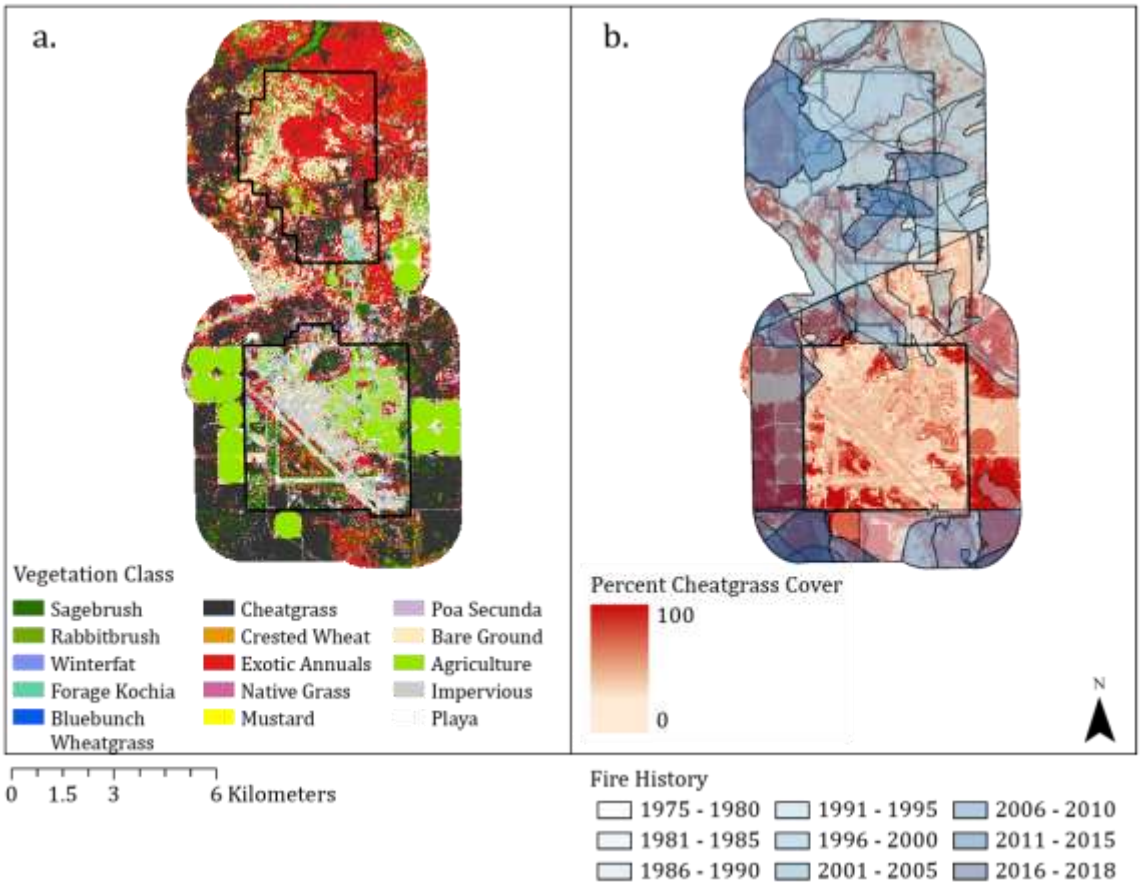

Figure 2.7 Vegetation classification of MHAFB Base and Small Arms Range (a); and corresponding cheatgrass cover (b) with fire history.

Saylor Creek Range is the largest of the MHAFB installations and has had the most disturbances from natural fire and training exercises. Crested wheatgrass has been mechanically planted in much of this range to try to combat the cheatgrass and this is clearly observed in the map (Figure 2.8a).

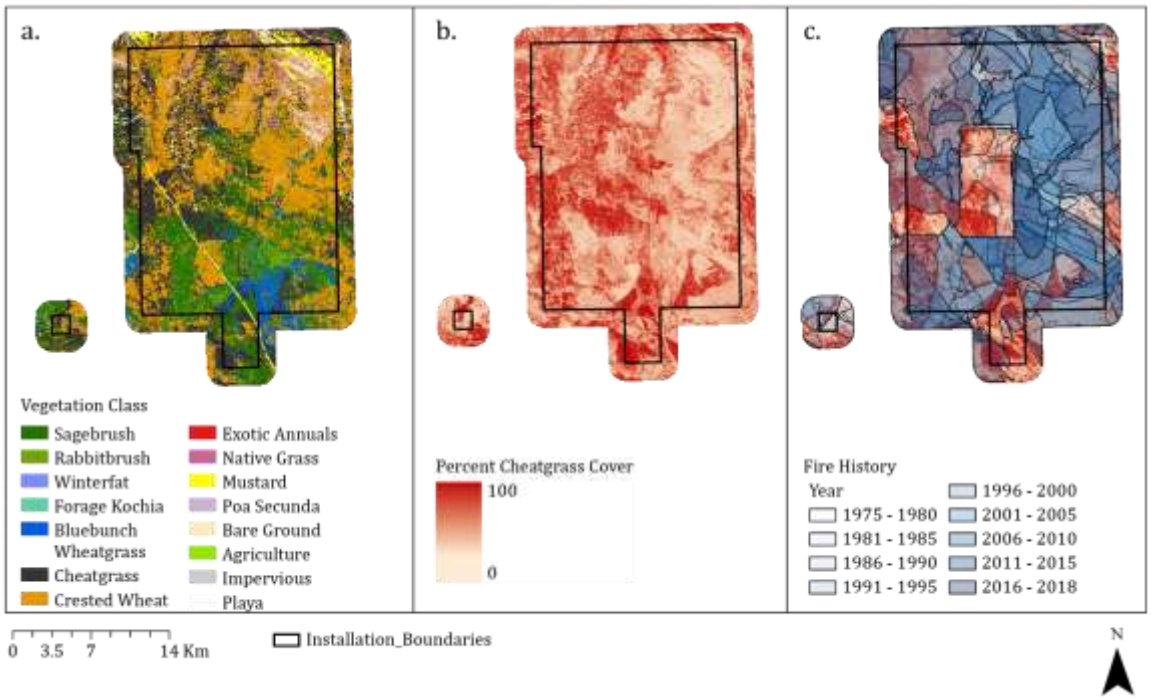

Figure 2.8 Vegetation classification of Saylor Creek Range (a); and corresponding cheatgrass cover (b) with fire history (c).

Juniper Butte Range has a higher elevation compared to other installations and has had few disturbances, leaving it the most intact range. The landscape is heterogenous, with a distribution of rabbitbrush, sagebrush and native grasses. The sharp boundary in the middle of the map is a fenced area where grazing is allowed on the south side.

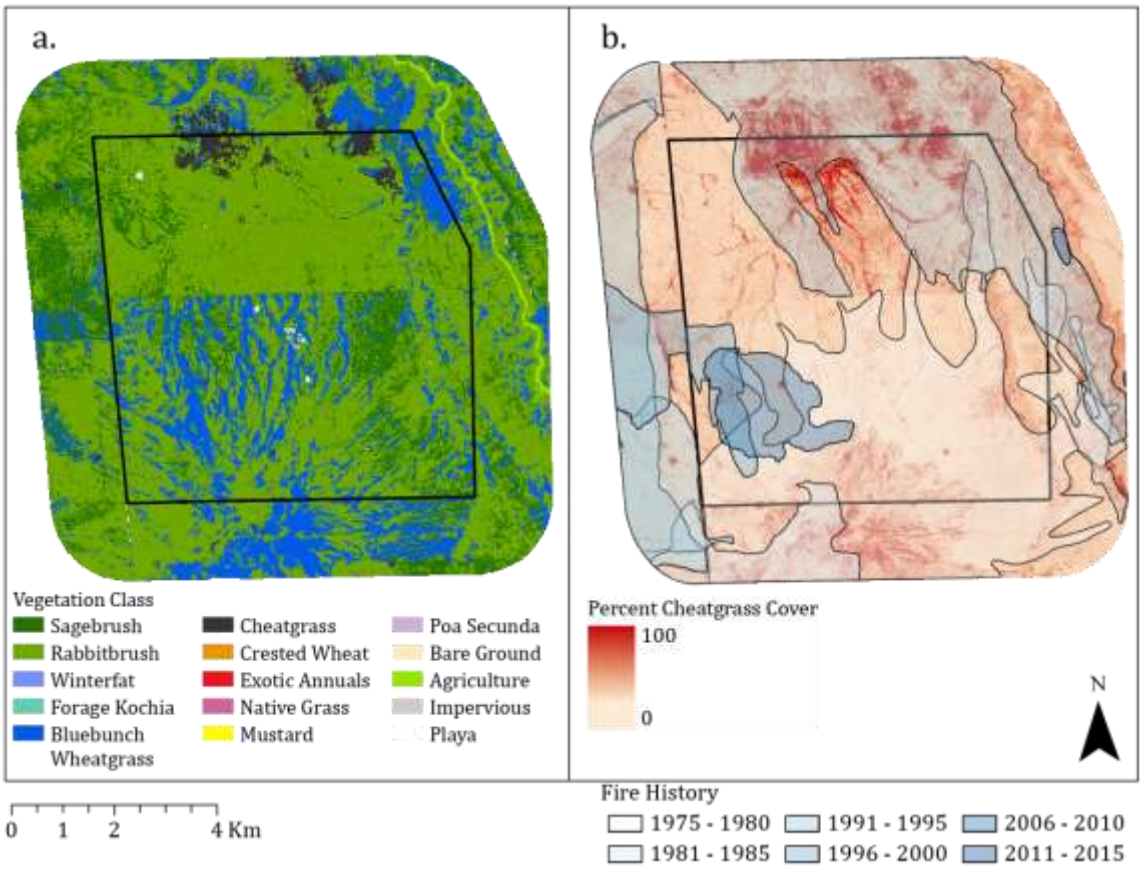

Figure 2.9 Vegetation classification of Juniper Butte Range (a); and corresponding cheatgrass cover (b) with fire history.

Figure 2.9b shows cheatgrass encroachment on Juniper Butte Range in the north end, where there was a fire. Figure 2.9a shows the area dominated by sagebrush and rabbitbrush but we know from Figure 2.9b there is a cheatgrass understory. The cheatgrass regression was of interest to land managers because they wanted to identify areas of encroachment before cheatgrass dominated the area. The R^2 of the cheatgrass regression is 0.58, with a Root Mean Square Error of 0.67%, and Mean Absolute Error of 11.8% (Figure 2.10).

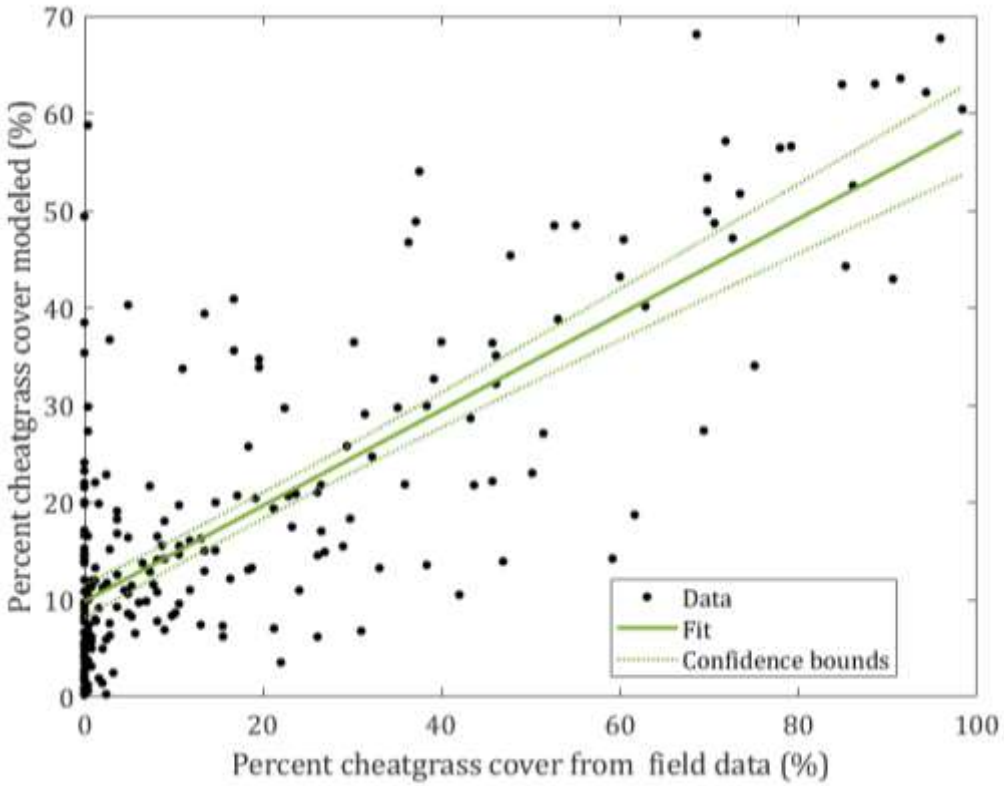

Figure 2.10 Cheatgrass percent cover from RF regression vs. field data (R^2 = 0.58).

Discussion

The combination of a vegetation classification and cheatgrass percent cover map provides detailed information for land managers to identify areas of native shrubs and areas of encroachment by cheatgrass. The 72.0% overall accuracy of the classification map is acceptable to our land management partners. Errors in the classification can be attributed to the heterogeneity of the ecosystem where 10 m spatial resolution results in mixed field plots for training and validation data, low signal to noise ratio, and spectral mixing in areas of abrupt vegetation change. This accuracy is relatively high for a heterogeneous dryland ecosystem, where pixels are inherently mixed, and across a large geographic area. Our overall accuracy for our classification with RF is slightly lower than Pelletier et al. (2016) who reported an overall accuracy of 83.3%; however, they

classified vegetation in agricultural fields (managed system). Our results for the cheatgrass regression showed an RMSE 0.67% which was lower compared to (Peterson, 2015) who reported RMSE values of 9.14% for their regression over Nevada. A potential source of error is the field data collection. The 5 photos used to determine percent cover for field plots only covered 1% of the plot area. More accurate assessments of vegetation cover, such as coverage from a UAV as described by Breckenridge et al. (2012) will improve the training data used.

The MHAFB Base and Small Arms Range have large amounts of cheatgrass close to many structures and houses, and few areas of sagebrush cover. Restoration efforts should work to remove cheatgrass and protect any current sagebrush to reduce fire frequency and risk (Bradley et al., 2018). Agriculture fields surrounding MHAFB Base and Small Arms Range were correctly classified but in the cheatgrass map some fields show a high percent cheatgrass cover while others show no understory of cheatgrass. The agriculture fields with cheatgrass understory have previously burned.

Saylor Creek Range is the target of wide swath (~150m) sprays of herbicides on cheatgrass. Crested wheatgrass was seeded throughout this range and dominates the northern half of the landscape. The cheatgrass map suggests there is an understory of cheatgrass in these areas. In fact, during field data collection we frequently observed seeded crested wheatgrass with an interspace of cheatgrass. This demonstrates the ability of the classification to pick out the spectral signal of the dominant vegetation in a co-dominated area. A yellow strip of tumble mustard runs from the west side to the southeast side of the map. This strip follows the main road that runs through the range and is not an artifact of the road but a validation of our classification because tumble mustard was

observed to grow within 10m on either side of the road. The southern half of the classification map shows areas dominated by sagebrush are adjacent to areas dominated by crested wheatgrass. The cheatgrass regression map in combination with the vegetation classification indicates that the areas of crested wheatgrass have a high percent cheatgrass. The patches of cheatgrass closely match previously burned areas on the range as shown in Figure 2.8b. Care should be taken to protect the sagebrush areas on Saylor Creek Range from burning because these areas likely would not recover. This range has a high amount of livestock grazing, and to conserve remaining sagebrush it is recommended to manage livestock grazing to support this conservation (Condon & Pyke, 2018; Davies et al., 2011).

At Juniper Butte Range, native rabbitbrush and sagebrush are the dominant species. In Figure 2.9 there appears to be a line through the middle of the range. This line is a fence through the range and was used as a fire break for a 1995 fire on the northern half of the range. Bluebunch wheatgrass was planted and spread throughout the southern half of the range after the 1980 fire. The 1995 fire and subsequent fire break stopped this spread of bluebunch wheatgrass. While Juniper Butte is the most intact range, the 1995 fire in the northern part of the range shows major cheatgrass encroachment. The classification map shows areas dominated by cheatgrass - these highly degraded areas are extremely hard to restore, and it is often more effective to identify where cheatgrass is spreading but is not yet the dominant vegetation (DiTomaso et al., 2010). The regression map shows exactly that; areas where cheatgrass is not yet dominant but encroaching. The classification map provides a complementary piece of information by indicating what vegetation the cheatgrass is encroaching on and where. Both maps are important for land

management, because they capture the gradient of vegetation and offer insights about the transition to an annual grass-dominated state.

The GEE code and workflow are open source and can be replicated in following years through collection of new training data and by changing the dates of the satellite imagery. To improve the classification and regression, we utilize Sentinel-2 Level 2 data corrected to surface reflectance instead of top of atmosphere. This may improve the overall accuracy because of the removal of atmospheric effects that have attenuated the surface reflectance signal. While some areas of Sentinel-2 Level 2 are available in GEE, there is not global coverage, although this is an available data product starting in 2020. Additionally, topography data such as a DEM and slope layer could be added as predictor variables to improve the classifier which is currently only based on spectral data (Franklin & Wulder, 2008). If available, more training data for sparse classes will improve the accuracy in the classification. The advent of unmanned aerial vehicles (UAVs) allows for field data collection of a large area in less time compared to a field crew (Gaston et al., 2018). UAV flights could be instrumental for collecting test and training data for landscape scale observations and provide imagery to develop a more accurate percent cover of vegetation for individual pixels (Breckenridge et al., 2012).

Future Work

While the cheatgrass regression map shows a range of 0-100%, work should be done to investigate the percent cover at which a spectral signal can be detected from a satellite. This threshold will likely be different based on the other vegetation in the pixel. Importantly, these thresholds would inform the uncertainty in areas of low percent cover cheatgrass. The time series of satellite imagery ranged from August 2017 - August of

2018. We did not use imagery after August 2018 due to a fire on the range that would have impacted the spectral signal. Future work should investigate different techniques such as including fire perimeters to mask out these areas and/or analyze the areas separately. The data from these maps can be implemented into fire models to better understand the interactions of fire and vegetation on a larger scale while maintaining a medium spatial resolution. Peeler et al. (2018) used models of cheatgrass cover to investigate the relationship of cheatgrass cover to fire history, fire frequency and severity across the entire Great Basin. Our cheatgrass cover map could be used to understand if these findings hold at a smaller spatial scale. Additionally, vegetation cover is an important parameter in modeling fire spread and severity. Pre-fire vegetation is a major predictor in post-fire vegetation growth, if an area was dominated by sagebrush but had a presence of cheatgrass pre-fire, Barker et al. (2019) found it was more likely to be dominated by exotic annuals post-fire. The regression and classification map can be used in predicting post-fire vegetation growth and combat invasive annual growth immediately following a fire.

CHAPTER THREE: ALLOMETRIC EQUATIONS FOR NON-NATIVE GRASSES USING EXTREMELY CLOSE-RANGE IMAGES AND STRUCTURE FROM MOTION

Introduction

Vegetation biomass is an important metric for assessing ecosystem structure, tracking vegetation growth, and quantifying carbon storage (Houghton & Hole, 2008). Semi-arid ecosystems act as carbon sinks and are thought to play a major role in global interannual carbon variations (Ahlström et al. 2015). There is a need to quantify above ground biomass (AGB) in semi-arid ecosystems to better understand their contribution to the global carbon flux, and the impacts of ecosystem shifts towards desertification (Chambers et al., 2014). AGB, defined as the dried weight of vegetation above the ground including both alive and dead components, is difficult to accurately measure in semi-arid ecosystems because of the heterogeneity and fine-scale structure of vegetation (Fern et al., 2018; Wijesingha et al., 2019).

The sagebrush steppe ecosystem is currently under threat from exotic annual grasses, such as cheatgrass (*Broumus Tectorum*) and medusahead (*Taeniatherum caput-medusae*), which are decreasing the biodiversity (Knapp, 1996), altering the fire cycle (Bradley et al., 2018), and reducing carbon storage (Bradley et al., 2006). AGB is an important metric for fire modeling, understanding fuel loads, and quantifying the effects of grazing on these threatened rangelands. In eastern Oregon, Davies et al. (2015) found dormant season grazing could decrease wildfire probability by decreasing fuel loads,

quantified by biomass measurements. Accurate AGB measurements at the plot scale can offer insights to land managers on the impacts of different grazing regimens on fuel load in the sagebrush steppe, while informing and validating AGB metrics derived at a landscape scale.

Current methods for collecting AGB can be described as a combination of site-specific and extrapolated measurements. An example of site-specific measurements is the destructive harvesting of biomass. Often quantification of biomass at the plot scale is extrapolated to larger scales (Clark et al., 2008). Further, in the field plot-level data collection of plants are destructively harvested, dried, and weighed to obtain a biomass metric, or point frame data is used to relate to biomass. The manual process itself has uncertainty in the collection from human error. Often these plots are small, and the biomass can vary significantly across spatial scales, even within 1 m or less. The act of removing plants itself alters the landscape and impacts future studies of those plots. Advances in remote sensing systems like lidar, unmanned aerial systems (UAS), and structure from motion (SfM) software have led to advances in quantifying biomass in dryland ecosystems (Anderson et al., 2018; Cunliffe et al., 2016). SfM is photogrammetry, the method of using 2D stereoscopic images and detecting common points, resulting in a 3D reconstruction in the form of a point cloud. SfM provides a similar data product to lidar - a point cloud in which vegetation structure can be interpreted. However since SfM is based on optical passive imagery it does not penetrate the canopy (Salamí et al., 2014). SfM and lidar are similar in their point cloud reconstruction, however, because lidar is active and it has an intensity associated with

each point. Additionally, lidar is often collected as full-waveform or in discrete returns which can characterize the understory.

In contrast SfM is derived from passive remote sensing relying on optical imagery to create point clouds where each point has an associated color value for the spectra of the optical image. This value is rarely radiometrically calibrated. SfM point clouds are not discretized from a waveform but developed based on the overlap of imagery taken. Vegetation parameters, like volume, can be derived from point clouds to develop allometric relationships between vegetation and destructively harvested biomass. SfM offers a low-cost, time efficient, and in some cases, more accurate method compared to terrestrial laser scanning (TLS) for estimating vegetation structure in dryland ecosystems (Olsoy et al., 2018; Wallace et al., 2017).

Extremely close-range SfM, defined by the use of hand-held instruments to collect the imagery for the SfM method, has shown success comparable to TLS in deriving parameters such as height and volume from the reconstruction of individual trees (Miller et al., 2015). In grasslands, extremely close-range SfM was shown to outperform TLS and traditional height measurements in developing allometric equations, in part because SfM can capture finer details compared to TLS, dependent upon the experimental setup (Cooper et al., 2017). SfM has been shown to successfully capture grasses and reconstruct fine features such as leaves and stems (Kröhnert et al., 2018). These previous studies demonstrate that SfM shows promise in providing accurate information for allometric equations used to extrapolate biomass of rangeland grass to a landscape-scale.

Allometric measurements relating point-cloud derived volumes have been developed for sagebrush using TLS point clouds and UAS (often referred to as close-range) SfM (Cunliffe et al., 2016; Li et al., 2015; Olsoy et al., 2014). Cunliffe et al. (2016) developed a reproduceable workflow for UAS data in the sagebrush steppe; grasses were assumed to be native perennial grasses and the allometric equation for black grama (*Bouteloua eriopoda*) was used in determining grass-dominated biomass. Anderson et al. (2018) used a machine learning algorithm to investigate TLS point cloud parameters for predicting exotic annual grasses, however this relationship cannot be applied outside of the study. To the author's knowledge allometric relationships of exotic annual grasses or non-native perennial grasses in the sagebrush steppe have not been developed for SfM volume and biomass. Allometric relationships have been developed for shrubs and trees in the sagebrush steppe but there is a need for relationships that include exotic annual grasses for the purpose of biomass quantification.

It is important to have biomass measurements of all plant functional types (PFT's), defined as groups of species that provide similar ecosystem functions, in the sagebrush steppe. Previous biomass studies in the sagebrush steppe have primarily focused on measurements of shrubs, forbs, perennial bunchgrasses and trees; biomass measurement of exotic grasses (both perennial and annual) are often neglected. This omission is problematic because exotic annuals were found to be present in 82% percent of the sagebrush steppe ecosystem in 2015 and continue to constitute a large percent of biomass (Boyte & Wylie, 2016). There is a need to quantify the AGB of exotic annual grasses for fuel load, forage availability, and carbon cycling. We aim to develop techniques for non-destructive SfM data collection of exotic annual grasses for the

purpose of AGB measurements. Due to the heterogenous nature of grasses we suggest a multi-species allometric relationship that includes exotic annual grasses to improve AGB estimates in the sagebrush steppe (Paul et al., 2013).

The objective of our work is to develop allometric relationships between SfM-derived volume and AGB in the sagebrush steppe. We are particularly interested in investigating this relationship in low elevation sagebrush steppe that has been invaded by exotic annual grasses. We test the ability of extremely close-range SfM to recreate mixed vegetation field plots (at the cm scale). Field work for capturing extremely close-range SfM imagery requires less training for field crews compared to TLS and UAS data collection and eliminates the need for specialized equipment. Developing an allometric relationship at a plot scale (cm) will inform future SfM studies that utilize UAS imagery (Gillan et al., 2020).

Research Questions

1. Can SfM imagery capture the structure of exotic grasses in low-elevation semi-arid ecosystems?
    a. If so, what relationship exists between SfM-derived volume and destructively harvested biomass measurements?
    b. What allometric relationship can be developed that includes native and exotic grasses in the sagebrush steppe?
2. How can biomass collection of heterogenous low elevation sagebrush steppe grasses be streamlined, as well as made affordable and easily reproducible?

Methods

Study Area: Three Fingers Allotment

The Three Fingers allotment located in southeastern Oregon (Figure 3.1) is a sagebrush steppe ecosystem and can be described as highly degraded with few shrubs present and an extensive cover of exotic annual grasses. Currently the Bureau of Land Management (BLM) manages the allotment which has a history of disturbance from grazing, recreation, and fire. Data collection was performed in 2019 by an Oregon State University and University of Idaho field crew in support of a USDA funded fine fuels project (Award #2019-68008-29914). Data collection took place on 3 different pastures– Camp Kettle, Saddle Butte, and McIntyre within each pasture a northern and southern exclosure was randomly placed, for a total of 6 treatment areas. Each exclosure contained 4 paddocks 150 m by 150 m in size.

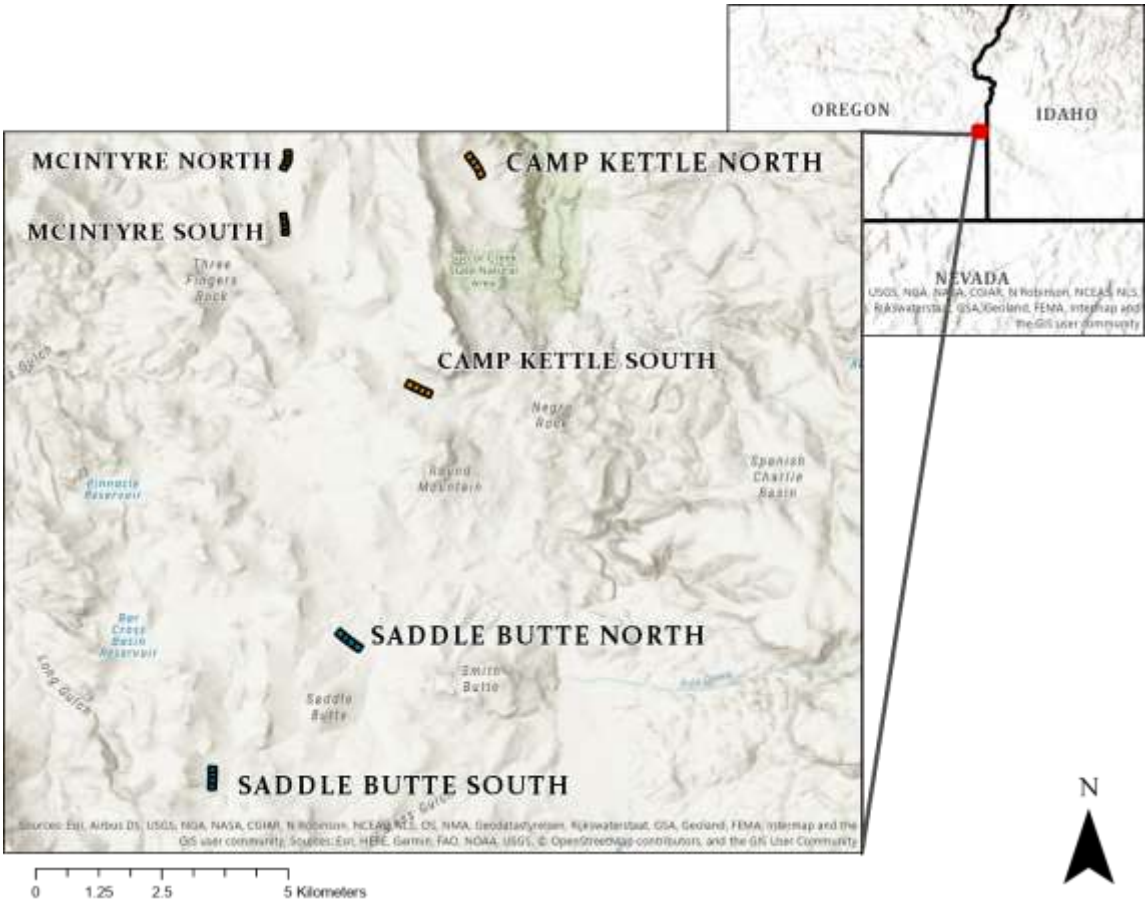

Figure 3.1 Three Fingers allotment and study exclosures

2019 Above Ground Biomass and SfM Data Collection

The protocol for the SfM data collection was designed to be efficient, minimize cost, and to coincide with rangeland data collection. In each paddock (n=24) the field crew took 3 transects at 25m, 50m and 75m from the fence. Along each transect line the field crew collected images for SfM and clipped biomass at 7m, 17m, 27m, 37m and 47m. To collect SfM images and AGB at each point along the transect, the field crew placed a ~40cm by 50cm Daubenmire frame. SfM data were initially collected with all destructively harvested AGB plots, but halfway through data collection SfM images were only taken at 7m, 27m, and 47m along the transect for a total data collection of n = 252. Approximately 30 images of the vegetation within and surrounding the frame were taken

with a Nikon CoolPix AW120 camera.

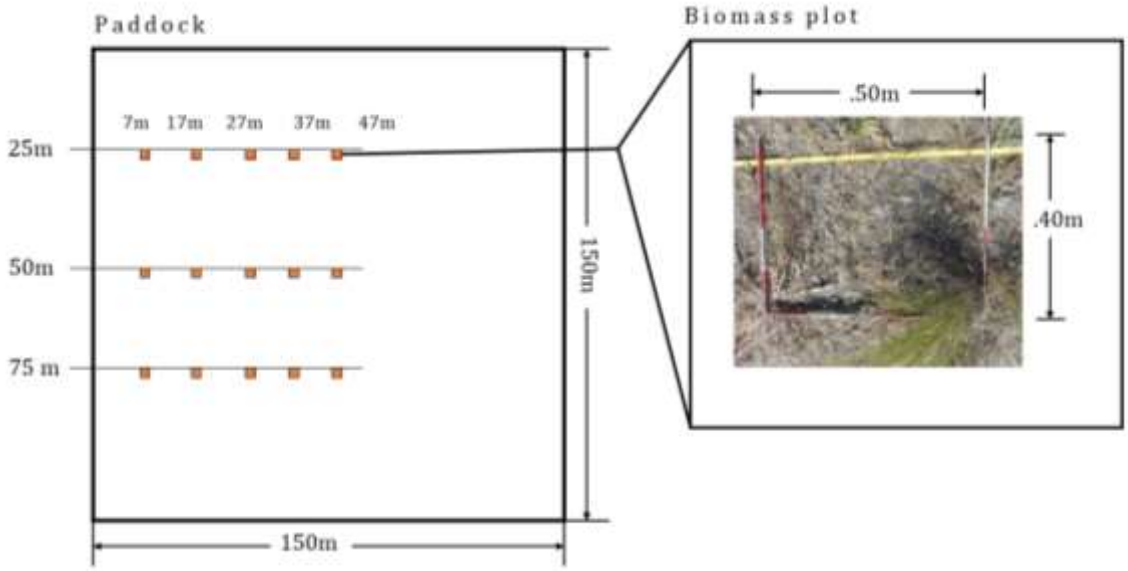

Figure 3.2 Schematic of transects in a paddock and biomass plot.

The camera was zoomed out and all images were taken with the camera oriented horizontally. After images were taken, the vegetation was destructively harvested and sorted into PFT's consisting of annual grass, perennial grass, forb, and litter. Vegetation was clipped at ground height and 2cm above ground for dense bunchgrasses. Vegetation was dried for 48 hours at 60ºC then weighed, initially reported in grams then divided by plot area (0.2 m^2) to be reported in g/m^2. A total of 252 SfM plots were collected out of a total of 360 biomass plots. The AGB distribution of plots used in the final analysis are shown in Figure 3.3a, litter made up most biomass collected, followed by annual grasses. Figure 3.3a does not have litter included as it was not used in the final analysis. Most plots contained exotic annual grasses (n=24), with only 13 plots containing perennial grasses (Figure 3.3b).

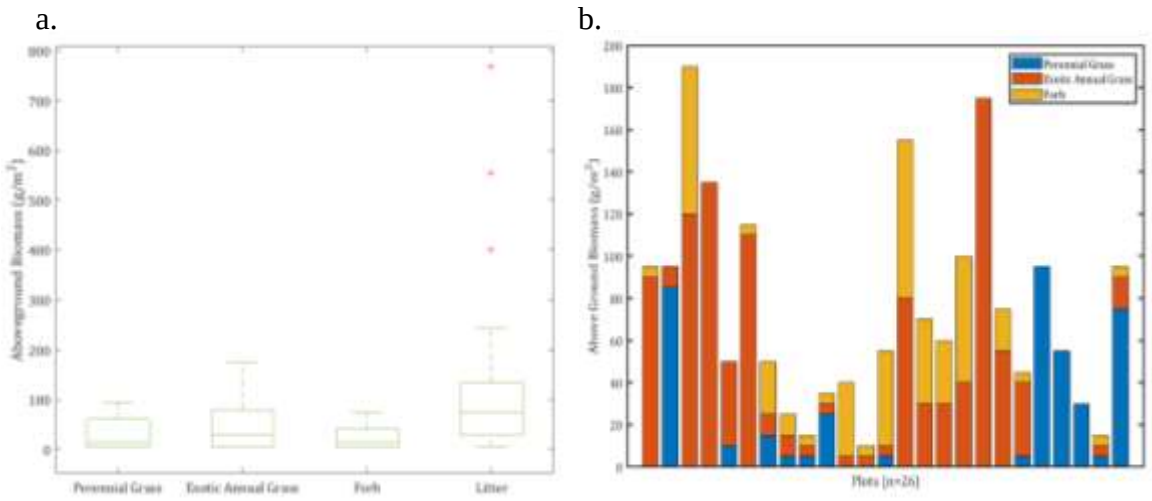

Figure 3.3 Distribution of dried AGB weights from plots used in final analysis (n=26).

SfM Photogrammetry Processing

We processed images using Agisoft Metashape Professional on Alienware computers with 2 GeForce RTX 2080 GPUs used to reduce processing time. The alignment settings used in Agisoft were *highest* and only *generic preselestion* was checked because everything was processed in local coordinates. When processing the image data, we found many of the images were of poor quality for SfM because of limited overlap between them (Figure 3.4). Image overlap of at least 60% is recommended for SfM reconstruction (Agisoft, 2020). Many images also contained people, horizon lines and human shadows that affected the post-processing.

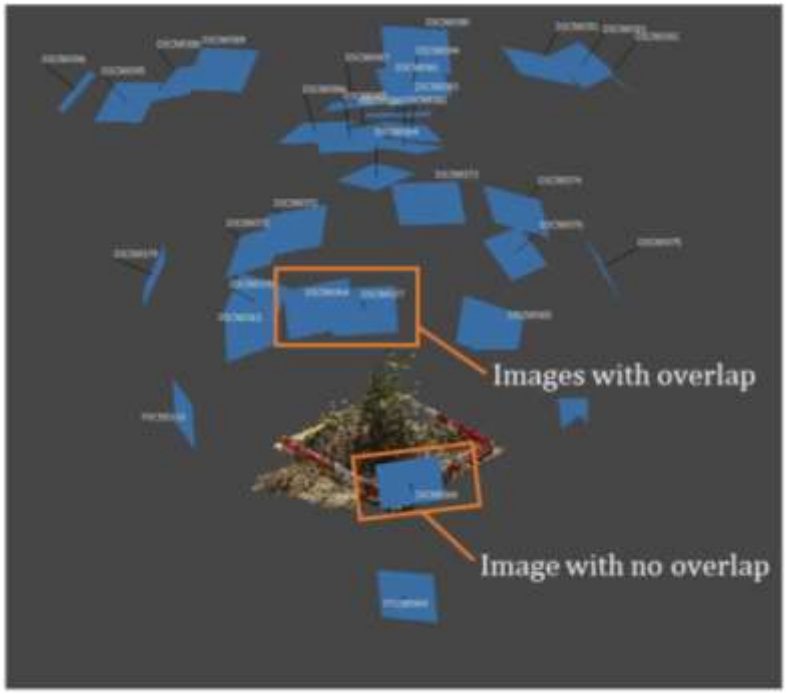

Figure 3.4 Examples of images with and without overlap used in image alignment in Agisoft.

In addition, if 20% of images did not align during the first alignment iteration in Agisoft, the plot was not further processed or used in AGB analysis. The 20% threshold was based on preliminary testing and analysis for data quality. We discarded 226 plots, leaving 26 plots which were processed to point clouds. In plots with 80% alignment, we manually added markers using the Daubenmire frame as a reference. A total of 11 markers were added to each plot to improve alignment of photos (see Appendix B).

Figure 3.5 SfM point cloud (left) derived from corresponding photo (right) used in reconstruction.

After markers were added the images were re-aligned with *reset current alignment*, *highest* and only *generic preselection*. Markers were used to add 4 scale bars in the Agisoft reference pane to provide the plot scale. Dense point clouds were created with *Ultra-High* quality and *Mild* depth filtering, point colors and confidence levels were checked. Local coordinates were added to markers to ensure that all point clouds were loaded and analyzed in the same reference frame. Dense point clouds were manually clipped to the surrounding Daubenmire frame, extraneous points were removed, and the point cloud was exported in local coordinates.

Volume Derived from SfM Point Clouds

A MATLAB script was developed to batch process the point clouds. Point clouds were clipped to a region of interest (ROI) defined by the Daubenmire frame and constrained by 4 cm below the frame in the vertical direction (Figure 3.6a). We used a volumetric surface differencing approach as described by Cooper et al. (2017) because SfM does not penetrate the canopy. The ground was determined by creating a coarse

mesh of 5 cm over the point cloud and finding the minimum elevation point within each cell as described in Wijesingha et al. (2019). This coarse mesh was resampled to a cell size of 0.5cm so the ground surface model was at the same resolution as the Digital Surface Model (DSM) (Figure 3.6b). To create the DSM a grid with a pixel size of 0.5 cm (Cooper et al., 2017) was overlaid on the point cloud. The highest elevation point within each cell was used to create the DSM. This grid was interpolated to fill any values that were empty with a natural neighbor interpolation (Figure 3.6c). The ground surface was subtracted from the DSM to create a Canopy Height Model (CHM) (Figure 3.6d). The height model was used to determine a volume (m^3) for each plot. The volume was associated with the destructively harvest biomass for each plot, shown in Appendix C.

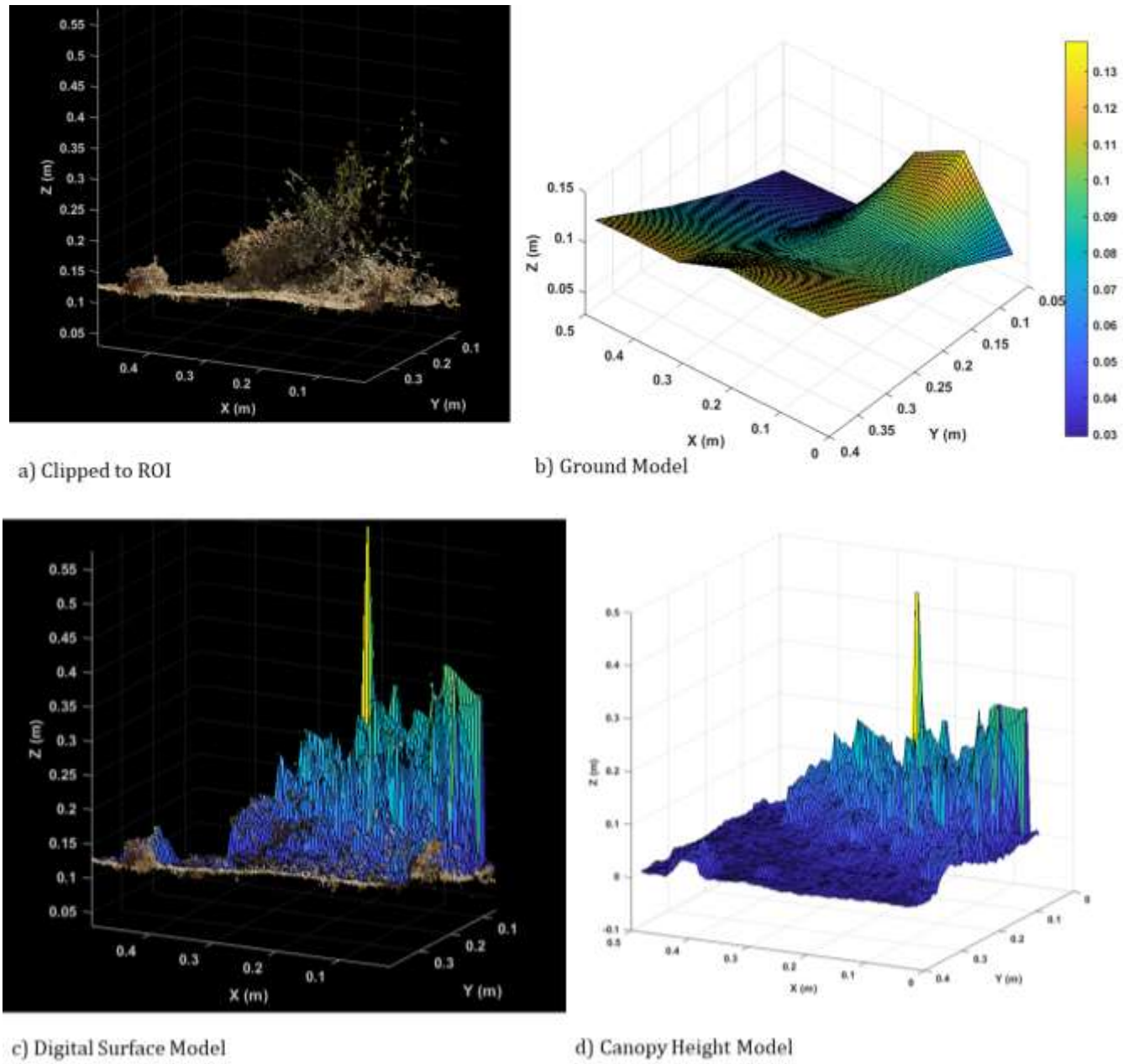

Figure 3.6 Workflow for SfM point cloud processing.

Regression Models

We used linear regression models to develop our mixed-plant functional type allometric equation. We compared field derived total AGB to SfM derived volume. Since litter was not resolved in the point clouds, it was subtracted from the total field derived AGB. However, since the variables do not follow a normal distribution (Figure 3.7), a natural log transformation of the variables was also investigated.

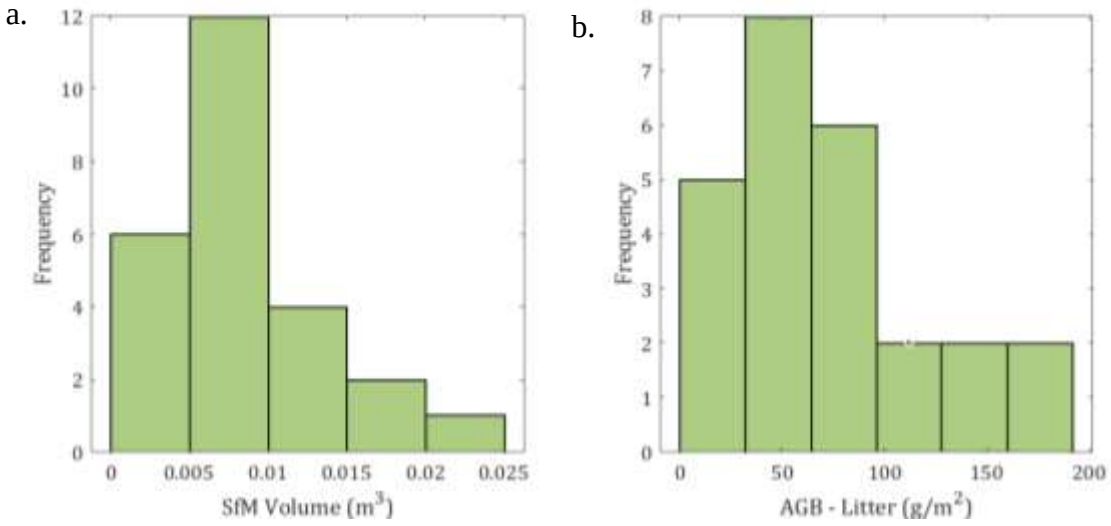

Figure 3.7 Distributions for SfM derived volume (a); and AGB minus litter (b).

Results

Allometric Regression Models

Using linear regression, we investigated a relationship between total AGB (g/m^2) and the SfM volume (m^3). We found no significant relationship with total AGB and SfM volume ($R^2 = 0.07$). We then investigated with SfM volume (m^3) and the total AGB minus litter (g/m^2) using the same approach. The linear regression with the total AGB adjusted for litter (g/m^2), had an R^2 of 0.43 and a Root Mean Square Error (RMSE) of 7.61g in a range of 2 to 38 g. The resulting allometric equation is AGB-Litter ~ 3.42 +

1343.3(SfM Volume). However, the residuals are not normally distributed and have a higher frequency of negative values, suggesting a log regression may better represent the data relationship (see Appendix D). As expected, transforming the variables to log space resulted in normally distributed residuals and improved the R^2 to 0.51 with an RMSE of 0.56g in a range of 0.69 to 3.64. The equation for the natural log transformed variables is thus ln(AGB - Litter) ~ 2.133+ 0.89 ln(SfM Volume).

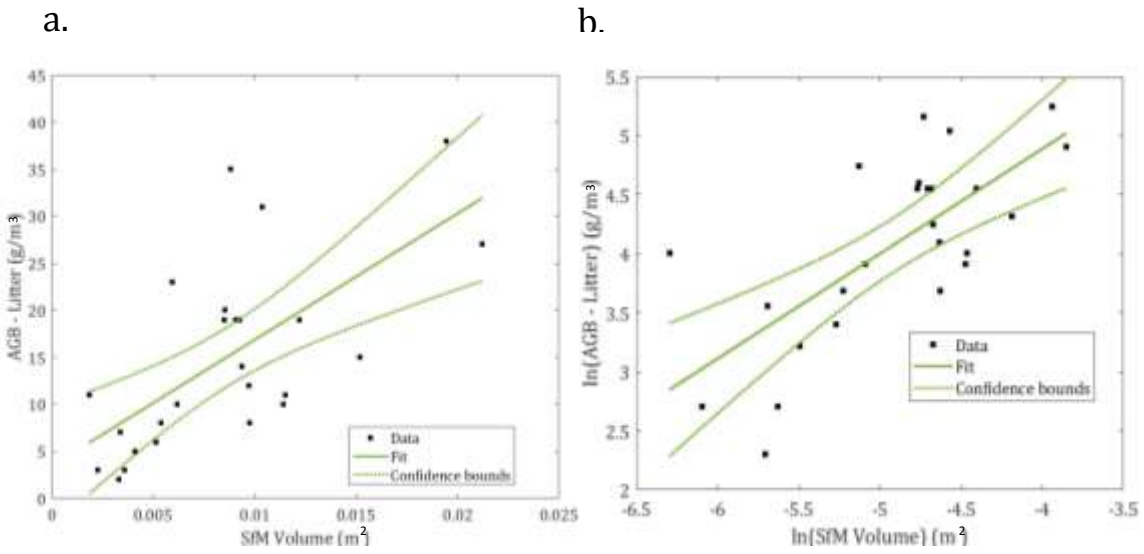

Figure 3.8 Linear regression of total AGB minus litter and SfM-derived Volume (a) compared to log-transformed linear regression (b).

Discussion

We found that the use of the non-destructive SfM method accurately estimated AGB in plots of mixed grasses, including annual and perennial, and forbs in low elevation sagebrush steppe ecosystems. Often a spectral classification is used to discriminate between PFT's or vegetation species before analysis (Akar et al., 2017; Gaston et al., 2018; Jing et al., 2017; Lu & He, 2017). Spectral data from images in this study were not used because they were not radiometrically corrected. Uncalibrated spectral parameters cannot be applicable to another study site or even to a different time

period in the same study site and were therefore omitted. In the sagebrush steppe, annual grasses are often mixed with perennial grasses and forbs and can be difficult to discriminate using spectral data alone, even with high spatial resolution UAS images (Gillan et al., 2020). With additional SfM field plots we could investigate models with individual PFT's to validate our assumption that a mixed PFT model will best represent the ecosystem. We expect our allometric equation to hold true for similar low elevation areas of sagebrush steppe with similar combinations of PFTs, and especially in highly degraded areas where non-native grasses were planted for restoration. This is because all perennial grasses in the study were non-native and we had a high amount of annual grasses in the training plots. Future work is needed to assess the extent to which this allometric equation can be used in other regions of the sagebrush steppe ecosystem.

SfM and point cloud reconstruction of grasses is difficult at any scale. At close-range (usually referring to UAS imagery) and extremely close-range (referring to handheld imagery) individual grasses are often too fine to discriminate in the reconstruction. Annual grasses are challenging in SfM. Their complex structure and heterogeneity provide little contrast between plants in the images, resulting in noisy point clouds (Agisoft, 2020; Miller et al., 2015). Visually, bunch grasses showed more success in reconstruction and less noise in the point clouds likely attributed to their distinct structure and the contrast in images with the surrounding bare ground. Sources of error can be attributed to the ground surface model, which often used points within the canopy of the bunch grass because the optical images, and thus SfM, cannot penetrate their dense bases. Other sources of error can be attributed to the manually added markers used for image registration in Agisoft. Since the markers were manually added to the Daubenmire

in Agisoft to align images, it is likely the markers were not on the same spot on the frame when added to each photo. Errors in image alignment are carried over to point cloud generation. We suggest the use of automatic markers be included in future close-range SfM studies to reduce error in image alignment, this would also decrease processing time in Agisoft. A revised field protocol for 2020 field data collection was informed from processing the 2019 data.

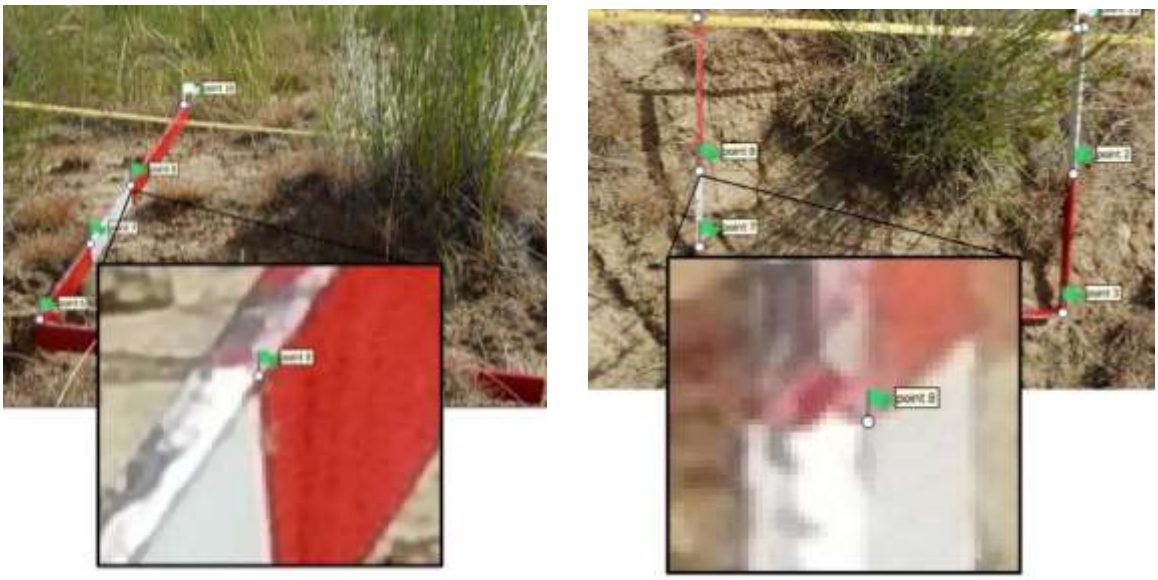

Figure 3.9 An example of marker/point 8 used in image alignment in two slightly different locations on the frame. This error will cause error in the point cloud reconstruction.

Many open-source tools used for SfM point cloud processing, such as LAStools, were developed to process lidar data. Software such as CloudCompare, Agisoft, and Pix4D are well suited for processing a few individual point clouds, like those created from UAS data through to volume measurements (Spreitzer et al., 2019; Wijesingha et al., 2019). However, we found it too time-intensive and computationally expensive to process more than approximately 20 individual point clouds using the software. Processing each point cloud independently also has the potential risk of inconsistency in

processing due to the introduction of human error. To reduce these issues, all data were processed using a batch script in MATLAB following a similar workflow to what the software provides, resulting in a final processing time of ~36 min to process all point clouds. This is remarkable given that our preliminary testing with other software would take more than 30 min per point cloud. This code can be used on future extremely close-range SfM datasets to minimize processing time and focus efforts on model development.

Linear regression models were used in previous studies in grasslands to relate biomass and structure (Wachendorf & Astor, 2019). In our dataset there were not enough structural differences to discriminate litter from the ground. SfM cannot penetrate litter and thus litter was often included in the ground surface model. This is shown in our poor relationship between SfM volume and biomass measurements that included litter. Since allometric equations are empirically based, we used the best-fit model while keeping the equation simple (Grinath, 2019). The resulting equation with an $R^2 = 0.51$ is comparable to results found by Grüner et al. (2019) in relating CHM derived from UAS SfM data to grass biomass $R^2 = 0.56$. Our equation is also comparable to Cooper et al. (2017) in their relationship between extremely close-range SfM volume and AGB of grass with an $R^2 = 0.54$. Their study also found they could not resolve the litter layer.

Further work is needed to investigate alternative methods for deriving volume, such as a convex hull, to see if the challenge associated with the litter layer can be resolved. Our residuals from our first model of biomass-litter to SfM volume showed an increase in error with an increase in volume, suggesting a log transform. A source of error with volumetric surface differencing is instances where vegetation is overhanging empty space. The code we used assumes the area under the highest point in the pixel is

filled with biomass and thus would overestimate the volume. Grass awns overhanging empty space were frequently observed in medusahead plots. To address the issue of counting empty space as biomass volume, the points in between the ground and vegetation surface could be used. Areas where the awns overlay empty space will have few points between the ground surface and vegetation height surface. In contrast, there should be more points defining the structure in areas where awns overlay biomass. This method would have issues with bunchgrasses where the canopy of awns is so dense the underlying stems are not captured in the point cloud. Future work is needed to find the most effective solution.

To improve and validate the model, additional high quality SfM plot data are needed. Often, plots with high error values had high AGB-litter measurements. Visual inspection of these plots found they were plots in which the vegetation was dense and thus had few ground points in the image reconstruction. In determining the ground surface, often vegetation points were misclassified as ground, leading to an underestimation of the volume. Determining the ground surface is a complex problem in processing both lidar and SfM point clouds. Grasses are often dense in cover and completely occlude the ground; it is recommended in SfM studies of grasses that ground control points be interspersed to verify the ground surface model as in Hillman et al. (2019).

Allometric equations of grasses derived from SfM have outperformed those derived from *in situ* measurements such as a disc pasture meter (Cooper et al., 2017). This could lead to large scale improvements in AGB estimates of grasses and forbs in the sagebrush steppe and improve the temporal resolution of these measurements. While

there are currently many UAS studies of the sagebrush steppe, the inclusion of AGB from annual grasses, non-native perennial grasses, and forbs will improve our understanding of this changing landscape.

CONCLUSIONS

The invasion of exotic annual grasses is dramatically altering the sagebrush steppe ecosystem. Remote sensing offers tools to researchers and land managers to understand the impact of exotic annual grasses at multiple scales, from the plot level to regional scales. Advances in cloud computing and machine learning when applied to satellite imagery offer accurate and reproducible workflows for mapping vegetation in semi-arid ecosystems. Mapping both dominate vegetation and percent cover for species of interest can offer land managers insight into areas susceptible to invasion and target areas for restoration. Structure from Motion can capture the structure and volume of mixed annual grasses and non-native perennial grasses to quantify above ground biomass. Accurate, non-destructive biomass measures of non-native grasses will help land managers quantify the impacts on fuel loads and forage quality, and help researchers understand the alterations to the carbon and Nitrogen cycles.

REFERENCES

Agisoft. (2020). Agisoft Metashape User Manual. *Agisoft Metashape*, *September*, 160. https://www.agisoft.com/pdf/metashape-pro_1_5_en.pdf

Ahlström, A., Michael R. Raupach, Guy Schurgers, Benjamin Smith, Almut Arneth, Martin Jung, Markus Reichstein, Josep G. Canadell, Pierre Friedlingstein, Atul K. Jain, Etsushi Kato, Benjamin Poulter, Stephen Sitch, Benjamin D. Stocker, N., & Viovy, Ying Ping Wang, Andy Wiltshire, S. Z. and N. Z. (2015). The dominant role of semi-arid ecosystems in the trend and variability of the land CO2 sink. *Journal of Geophysical Research: Space Physics*, *120*(6), 895–899. https://doi.org/10.1126/science.aaa1668

Akar, A., Gökalp, E., Akar, & Yılmaz, V. (2017). Improving classification accuracy of spectrally similar land covers in the rangeland and plateau areas with a combination of WorldView-2 and UAV images. *Geocarto International*, *32*(9), 990–1003. https://doi.org/10.1080/10106049.2016.1178816

Anderson, K. E., Glenn, N. F., Spaete, L. P., Shinneman, D. J., Pilliod, D. S., Arkle, R. S., McIlroy, S. K., & Derryberry, D. W. R. (2018). Estimating vegetation biomass and cover across large plots in shrub and grass dominated drylands using terrestrial lidar and machine learning. *Ecological Indicators*, *84*(January 2017), 793–802. https://doi.org/10.1016/j.ecolind.2017.09.034

Barker, B. S., Pilliod, D. S., Rigge, M., & Homer, C. G. (2019). Pre-fire vegetation drives post-fire outcomes in sagebrush ecosystems: evidence from field and remote sensing data. *Ecosphere*, *10*(11). https://doi.org/10.1002/ecs2.2929

Belgiu, M., & Drăgu, L. (2016). Random forest in remote sensing: A review of applications and future directions. In *ISPRS Journal of Photogrammetry and Remote Sensing* (Vol. 114, pp. 24–31). Elsevier B.V. https://doi.org/10.1016/j.isprsjprs.2016.01.011

Boyte, S. P., & Wylie, B. K. (2016). Near-Real-Time Cheatgrass Percent Cover in the Northern Great Basin, USA, 2015. *Rangelands*, *38*(5), 278–284. https://doi.org/10.1016/j.rala.2016.08.002

Boyte, S. P., Wylie, B. K., & Major, D. J. (2015). Mapping and monitoring cheatgrass dieoff in rangelands of the Northern Great Basin, USA. *Rangeland Ecology and Management*, *68*(1), 18–28. https://doi.org/10.1016/j.rama.2014.12.005

Boyte, S. P., Wylie, B. K., & Major, D. J. (2016). Cheatgrass percent cover change: Comparing recent estimates to climate change - Driven predictions in the Northern Great Basin. *Rangeland Ecology and Management*, *69*(4), 265–279. https://doi.org/10.1016/j.rama.2016.03.002

Bradley, B. A., Curtis, C. A., Fusco, E. J., Abatzoglou, J. T., Balch, J. K., Dadashi, S., & Tuanmu, M.-N. (2018). Cheatgrass (Bromus tectorum) distribution in the intermountain Western United States and its relationship to fire frequency, seasonality, and ignitions. *Biological Invasions*, *20*(6), 1493–1506. https://doi.org/10.1007/s10530-017-1641-8

Bradley, B. A., Houghton, R. A., Mustard, J. F., & Hamburg, S. P. (2006). Invasive grass reduces aboveground carbon stocks in shrublands of the Western US. *Global Change Biology*, *12*(10), 1815–1822. https://doi.org/10.1111/j.1365-2486.2006.01232.x

Breckenridge, R. P., Dakins, M., Bunting, S., Harbour, J. L., & Lee, R. D. (2012). Using Unmanned Helicopters to Assess Vegetation Cover in Sagebrush Steppe Ecosystems. *Rangeland Ecology & Management*, *65*(4), 362–370. https://doi.org/10.2111/REM-D-10-00031.1

Chambers, J. C., Bradley, B. A., Brown, C. S., D'Antonio, C., Germino, M. J., Grace, J. B., Hardegree, S. P., Miller, R. F., & Pyke, D. A. (2014). Resilience to Stress and Disturbance, and Resistance to Bromus tectorum L. Invasion in Cold Desert Shrublands of Western North America. *Ecosystems*, *17*(2), 360–375. https://doi.org/10.1007/s10021-013-9725-5

Clark, P. E., Hardegree, S. P., Moffet, C. A., & Pierson, F. B. (2008). Point sampling to

stratify biomass variability in sagebrush steppe vegetation. *Rangeland Ecology and Management*, *61*(6), 614–622. https://doi.org/10.2111/07-147.1

Clinton, N. E., Potter, C., Crabtree, B., Genovese, V., Gross, P., Gong, P., Gross, P., Clinton, N. E., Crabtree, B., Genovese, V., Potter, C., Crabtree, B., Genovese, V., Gross, P., & Gong, P. (2010). Remote Sensing–Based Time-Series Analysis of Cheatgrass (L.) Phenology. *Journal of Environment Quality*, *39*(3), 955. https://doi.org/10.2134/jeq2009.0158

Condon, L. A., & Pyke, D. A. (2018). Fire and Grazing Influence Site Resistance to Bromus tectorum Through Their Effects on Shrub, Bunchgrass and Biocrust Communities in the Great Basin (USA). *Ecosystems*, *21*(7), 1416–1431. https://doi.org/10.1007/s10021-018-0230-8

Cooper, S. D., Roy, D. P., Schaaf, C. B., & Paynter, I. (2017). Examination of the potential of terrestrial laser scanning and structure-from-motion photogrammetry for rapid nondestructive field measurement of grass biomass. *Remote Sensing*, *9*(6). https://doi.org/10.3390/rs9060531

Cunliffe, A. M., Brazier, R. E., & Anderson, K. (2016). Remote Sensing of Environment Ultra- fi ne grain landscape-scale quanti fi cation of dryland vegetation structure with drone-acquired structure-from-motion photogrammetry. *Remote Sensing of Environment*, *183*, 129–143. https://doi.org/10.1016/j.rse.2016.05.019

Davies, K. W., Boyd, C. S., Bates, J. D., & Hulet, A. (2015). Dormant season grazing may decrease wildfire probability by increasing fuel moisture and reducing fuel amount and continuity. *International Journal of Wildland Fire*, *24*(6), 849–856. https://doi.org/10.1071/WF14209

Davies, K. W., Boyd, C. S., Beck, J. L., Bates, J. D., Svejcar, T. J., & Gregg, M. A. (2011). Saving the sagebrush sea: An ecosystem conservation plan for big sagebrush plant communities. *Biological Conservation*, *144*(11), 2573–2584. https://doi.org/10.1016/j.biocon.2011.07.016

DiTomaso, J. M., Masters, R. A., & Peterson, V. F. (2010). Rangeland Invasive Plant Management. *Rangelands*, *32*(1), 43–47. https://doi.org/10.2111/RANGELANDS-

D-09-00007.1

Drusch, M., Del Bello, U., Carlier, S., Colin, O., Fernandez, V., Gascon, F., Hoersch, B., Isola, C., Laberinti, P., Martimort, P., Meygret, A., Spoto, F., Sy, O., Marchese, F., & Bargellini, P. (2012). Sentinel-2: ESA's Optical High-Resolution Mission for GMES Operational Services. *Remote Sensing of Environment, 120*, 25–36. https://doi.org/10.1016/J.RSE.2011.11.026

Enterkine, J. (2019). Remote Sening Time-Series Analsis, Machine Learning, and K-Means Clustering Imporves Dryland Vegetation and Biological Soil Crust. *Boise State University Theses and Dissertations*. 1523. https://doi.org/10.1017/CBO9781107415324.004

Fern, R. R., Foxley, E. A., Bruno, A., & Morrison, M. L. (2018). Suitability of NDVI and OSAVI as estimators of green biomass and coverage in a semi-arid rangeland. *Ecological Indicators*, *94*(June), 16–21. https://doi.org/10.1016/j.ecolind.2018.06.029

Fitzgerald, G., Rodriguez, D., & O'Leary, G. (2010). Measuring and predicting canopy nitrogen nutrition in wheat using a spectral index-The canopy chlorophyll content index (CCCI). *Field Crops Research*, *116*(3), 318–324. https://doi.org/10.1016/j.fcr.2010.01.010

Forster, M., Schmidt, T., Wolf, R., Kleinschmit, B., Fassnacht, F. E., Cabezas, J., & Kattenborn, T. (2017). Detecting the spread of invasive species in central Chile with a Sentinel-2 time-series. *2017 9th International Workshop on the Analysis of Multitemporal Remote Sensing Images, MultiTemp 2017*, 4–7. https://doi.org/10.1109/Multi-Temp.2017.8035216

Franklin, S. E., & Wulder, M. A. (2008). Progress in Physical Geography Remote sensing methods in medium spatial resolution satellite data land cover classification of large areas. *Progress in Physical Geography, 2*, 173–205. https://doi.org/10.1191/0309133302pp332ra

Gallagher, M. (2018). Utilizing Satellite Fusion Methods to Assess Vegetation Phenology in a Semi-Arid Ecosystem. *Boise State University Theses and Dissertations*. 1425.

https://doi.org/10.18122/td/1425/boisestate

Gaston, K. J., Gonzalez, F., Mengersen, K., Gaston, K. J., Sandino, J., Gonzalez, F., Mengersen, K., & Gaston, K. J. (2018). UAVs and Machine Learning Revolutionising Invasive Grass and Vegetation Surveys in Remote Arid Lands. *Sensors*, *18*(2), 605. https://doi.org/10.3390/s18020605

Gillan, J. K., Karl, J. W., & van Leeuwen, W. J. D. (2020). Integrating drone imagery with existing rangeland monitoring programs. *Environmental Monitoring and Assessment*, *192*(5). https://doi.org/10.1007/s10661-020-8216-3

Gitelson, A. A., Merzlyak, M. N., & Chivkunova, O. B. (2001). Optical Properties and Nondestructive Estimation of Anthocyanin Content in Plant Leaves¶. *Photochemistry and Photobiology*, *74*(1), 38. https://doi.org/10.1562/0031-8655(2001)074<0038:opaneo>2.0.co;2

Gorelick, N., Hancher, M., Dixon, M., Ilyushchenko, S., Thau, D., & Moore, R. (2017). Google Earth Engine: Planetary-scale geospatial analysis for everyone. *Remote Sensing of Environment*, *202*, 18–27. https://doi.org/10.1016/j.rse.2017.06.031

Grinath, J. B. (2019). Comparing predictive measures and model functions for estimating plant biomass: lessons from a sagebrush–rabbitbrush community. *Plant Ecology*, *220*(6), 619–632. https://doi.org/10.1007/s11258-019-00940-1

Grüner, E., Astor, T., & Wachendorf, M. (2019). Biomass prediction of heterogeneous temperate grasslands using an SFM approach based on UAV imaging. *Agronomy*, *9*(2). https://doi.org/10.3390/agronomy9020054

Gurung, R. B., Breidt, F. J., Dutin, A., & Ogle, S. M. (2009). Predicting Enhanced Vegetation Index (EVI) curves for ecosystem modeling applications. *Remote Sensing of Environment*, *113*(10), 2186–2193. https://doi.org/10.1016/j.rse.2009.05.015

Hillman, S., Wallace, L., Reinke, K., Hally, B., Jones, S., & Saldias, D. S. (2019). A method for validating the structural completeness of understory vegetation models captured with 3D remote sensing. *Remote Sensing*, *11*(18). https://doi.org/10.3390/rs11182118

Houghton, R. A., & Hole, W. (2008). Quantities of Biomass Importance. *Small*, *1990*, 448–453.

Jing, R., Gong, Z., Zhao, W., Pu, R., & Deng, L. (2017). Above-bottom biomass retrieval of aquatic plants with regression models and SfM data acquired by a UAV platform – A case study in Wild Duck Lake Wetland, Beijing, China. *ISPRS Journal of Photogrammetry and Remote Sensing*, *134*, 122–134. https://doi.org/10.1016/j.isprsjprs.2017.11.002

Jones, M. O., Allred, B. W., Naugle, D. E., Maestas, J. D., Donnelly, P., Metz, L. J., Karl, J., Smith, R., Bestelmeyer, B., Boyd, C., Kerby, J. D., & McIver, J. D. (2018). Innovation in rangeland monitoring: annual, 30 m, plant functional type percent cover maps for U.S. rangelands, 1984–2017. *Ecosphere*, *9*(9). https://doi.org/10.1002/ecs2.2430

Knapp, P. A. (1996). Cheatgrass (Bromus tectorum L) dominance in the great basin desert. History, persistence, and influences to human activities. *Global Environmental Change*, *6*(1), 37–52. https://doi.org/10.1016/0959-3780(95)00112-3

Kröhnert, M., Anderson, R., Bumberger, J., Dietrich, P., Harpole, W. S., & Maas, H. G. (2018). Watching grass grow - A pilot study on the suitability of photogrammetric techniques for quantifying change in Aboveground Biomass in Grassland experiments. *International Archives of the Photogrammetry, Remote Sensing and Spatial Information Sciences - ISPRS Archives*, *42*(2), 539–542. https://doi.org/10.5194/isprs-archives-XLII-2-539-2018

Kumar, L., Mutanga, O., Kumar, L., & Mutanga, O. (2018). Google Earth Engine Applications Since Inception: Usage, Trends, and Potential. *Remote Sensing*, *10*(10), 1509. https://doi.org/10.3390/rs10101509

Li, A., Glenn, N. F., Olsoy, P. J., Mitchell, J. J., & Shrestha, R. (2015). Aboveground biomass estimates of sagebrush using terrestrial and airborne LiDAR data in a dryland ecosystem. *Agricultural and Forest Meteorology*, *213*, 138–147. https://doi.org/10.1016/j.agrformet.2015.06.005

Lu, B., & He, Y. (2017). Species classification using Unmanned Aerial Vehicle (UAV)-

acquired high spatial resolution imagery in a heterogeneous grassland. *ISPRS Journal of Photogrammetry and Remote Sensing*, *128*, 73–85. https://doi.org/10.1016/j.isprsjprs.2017.03.011

Miller, J., Morgenroth, J., & Gomez, C. (2015). 3D modelling of individual trees using a handheld camera: Accuracy of height, diameter and volume estimates. *Urban Forestry and Urban Greening*, *14*(4), 932–940. https://doi.org/10.1016/j.ufug.2015.09.001

Moriarty, K., Okesen, L., & Pellant, M. (2015). Fuel Breaks that Work. *Great Basin Factsheet*, *5*, 1–6.

Olsoy, P. J., Glenn, N. F., Clark, P. E., & Derryberry, D. W. R. (2014). Aboveground total and green biomass of dryland shrub derived from terrestrial laser scanning. *ISPRS Journal of Photogrammetry and Remote Sensing*, *88*, 166–173. https://doi.org/10.1016/j.isprsjprs.2013.12.006

Olsoy, P. J., Shipley, L. A., Rachlow, J. L., Forbey, J. S., Glenn, N. F., Burgess, M. A., & Thornton, D. H. (2018). Unmanned aerial systems measure structural habitat features for wildlife across multiple scales. *Methods in Ecology and Evolution*, *9*(3), 594–604. https://doi.org/10.1111/2041-210X.12919

Panigada, C., Tagliabue, G., Zaady, E., Lezion, R., Garzonio, R., & Cogliati, S. (2019). *A new approach for biocrust and vegetation monitoring in drylands using multi-temporal Sentinel-2 images*. https://doi.org/10.1177/0309133319841903

Paul, K. I., Roxburgh, S. H., England, J. R., Ritson, P., Hobbs, T., Brooksbank, K., John Raison, R., Larmour, J. S., Murphy, S., Norris, J., Neumann, C., Lewis, T., Jonson, J., Carter, J. L., McArthur, G., Barton, C., & Rose, B. (2013). Development and testing of allometric equations for estimating above-ground biomass of mixed-species environmental plantings. *Forest Ecology and Management*, *310*, 483–494. https://doi.org/10.1016/j.foreco.2013.08.054

Pavlov, Y. L. (2019). Random forests. *Random Forests*, 1–122. https://doi.org/10.1201/9780429469275-8

Peeler, J. L., & Smithwick, E. A. H. (2018). Exploring invasibility with species

distribution modeling: How does fire promote cheatgrass (Bromus tectorum) invasion within lower montane forests? *Diversity and Distributions*, *24*(9), 1308–1320. https://doi.org/10.1111/ddi.12765

Pelletier, C., Valero, S., Inglada, J., Champion, N., & Dedieu, G. (2016). Assessing the robustness of Random Forests to map land cover with high resolution satellite image time series over large areas. *Remote Sensing of Environment*, *187*, 156–168. https://doi.org/10.1016/j.rse.2016.10.010

Peterson, E. B. (2015). *Mapping Percent-Cover of the Invasive Species Bromus tectorum (Cheatgrass) over a Large Portion of Nevada from Satellite Imagery . January 2003*.

Poulter, B., Frank, D., Ciais, P., Myneni, R. B., Andela, N., Bi, J., Broquet, G., Canadell, J. G., Chevallier, F., Liu, Y. Y., Running, S. W., Sitch, S., & Van Der Werf, G. R. (2014). Contribution of semi-arid ecosystems to interannual variability of the global carbon cycle. *Nature*, *509*(7502), 600–603. https://doi.org/10.1038/nature13376

Rouse, J. W., Hass, R. H., Schell, J. A., & Deering, D. W. (1973). Monitoring vegetation systems in the great plains with ERTS. *Third Earth Resources Technology Satellite (ERTS) Symposium*, *1*, 309–317. https://doi.org/citeulike-article-id:12009708

Salamí, E., Barrado, C., & Pastor, E. (2014). UAV flight experiments applied to the remote sensing of vegetated areas. *Remote Sensing*, *6*(11), 11051–11081. https://doi.org/10.3390/rs61111051

Smith, W. K., Dannenberg, M. P., Yan, D., Herrmann, S., Barnes, M. L., Barron-gafford, G. A., Biederman, J. A., Ferrenberg, S., Fox, A. M., Hudson, A., Knowles, J. F., Macbean, N., Moore, D. J. P., Nagler, P. L., Reed, S. C., Rutherford, W. A., Scott, R. L., Wang, X., & Yang, J. (2019). Remote Sensing of Environment Remote sensing of dryland ecosystem structure and function : Progress , challenges , and opportunities. *Remote Sensing of Environment*, *233*(August), 111401. https://doi.org/10.1016/j.rse.2019.111401

Spaete, L. P., Glenn, N. F., & Baun, C. W. (2016). *Morley Nelson Snake River Birds of Prey National Conservation Area 2013 RapidEye 7m Landcover Classification*.

Spreitzer, G., Tunnicliffe, J., & Friedrich, H. (2019). Using Structure from Motion photogrammetry to assess large wood (LW) accumulations in the field. *Geomorphology*. https://doi.org/10.1016/j.geomorph.2019.106851

Van Gunst, K. J., Baughman, O. W., Cleeves, L., Meyer, S. E., Dilts, T. E., Leger, E. A., & Weisberg, P. J. (2017). Development of remote sensing indicators for mapping episodic die-off of an invasive annual grass (Bromus tectorum) from the Landsat archive. *Ecological Indicators*, *79*(March), 173–181. https://doi.org/10.1016/j.ecolind.2017.04.024

Wachendorf, M., & Astor, T. (2019). The benefit of spectral and point-cloud data for herbage yield and quality assessment of grasslands. *International Archives of the Photogrammetry, Remote Sensing and Spatial Information Sciences - ISPRS Archives*, *42*(2/W16), 267–272. https://doi.org/10.5194/isprs-archives-XLII-2-W16-267-2019

Wallace, L., Hillman, S., Reinke, K., & Hally, B. (2017). Non-destructive estimation of above-ground surface and near-surface biomass using 3D terrestrial remote sensing techniques. *Methods in Ecology and Evolution*, *8*(11), 1607–1616. https://doi.org/10.1111/2041-210X.12759

West, A. M., Evangelista, P. H., Jarnevich, C. S., Kumar, S., Swallow, A., Luizza, M. W., & Chignell, S. M. (2017). Using multi-date satellite imagery to monitor invasive grass species distribution in post-wildfire landscapes: An iterative, adaptable approach that employs open-source data and software. *International Journal of Applied Earth Observation and Geoinformation*, *59*, 135–146. https://doi.org/10.1016/j.jag.2017.03.009

Wijesingha, J., Moeckel, T., Hensgen, F., & Wachendorf, M. (2019). Evaluation of 3D point cloud-based models for the prediction of grassland biomass. *International Journal of Applied Earth Observation and Geoinformation*, *78*(May 2018), 352–359. https://doi.org/10.1016/j.jag.2018.10.006

Ziska, L. H., Reeves, J. B., & Blank, B. (2005). The impact of recent increases in atmospheric CO2 on biomass production and vegetative retention of Cheatgrass

(Bromus tectorum): Implications for fire disturbance. *Global Change Biology*, *11*(8), 1325–1332. https://doi.org/10.1111/j.1365-2486.2005.00992.x

APPENDIX A

Survey 123 Survey Questions

Plot Number
Location on MHAFB Installation
RTK taken?
Date
Image facing North: {Image from the center of the plot facing north}
Image facing East: {Image from the center of the plot facing north}
Image facing South: {Image from the center of the plot facing north}
Image facing West: {Image from the center of the plot facing north}
Center Photoplot #?
North Photoplot #?
East Photoplot #?
South Photoplot #?
West Photoplot #?
Dominant species?
Second Dominant Species Percentage?
Third Dominant Species Percentage?
Fourth Dominat Species Percentage?
Shrubs Present?
Shrub Species
Grass Present?
Grass Species
Forbes Present?
Forbes Species:
Exotics Present?
Exotic Species:
ID Noxious Weeds Present?
Others?
Any Notes?
Location

APPENDIX B

Schematic of Daubenmire Frame and Markers Placed in Agisoft

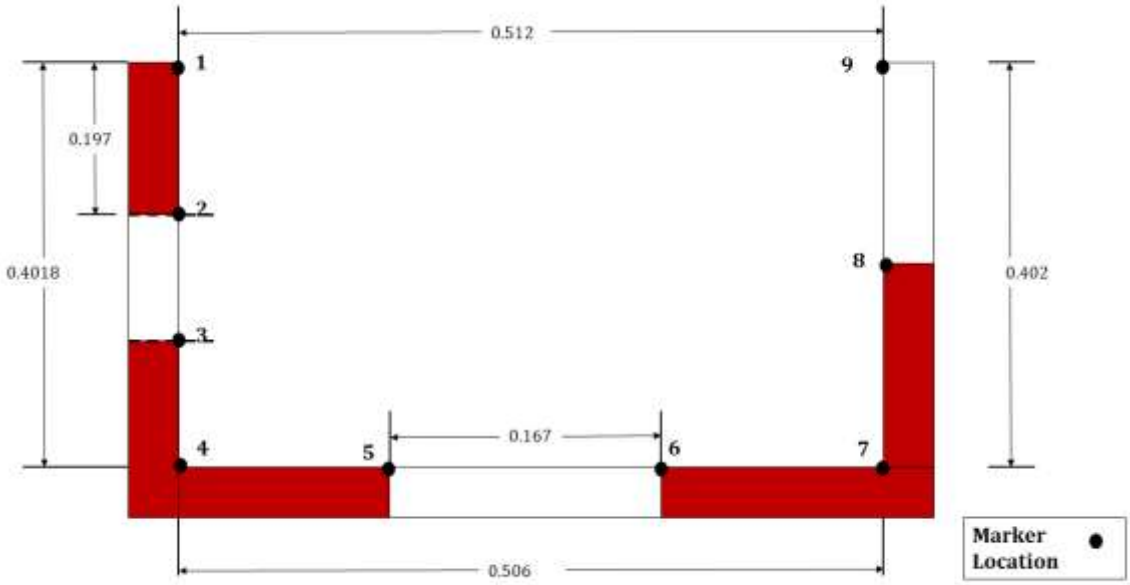
0.512
1
9
0.197
2
0.4018
8
0.402
3
0.167
4
5
6
7
0.506
Marker Location

APPENDIX C

Table of AGB and SfM Volume

Destructively Harvested Biomass (g)						SfM Volume (m^3)
Annual Grass	Perennial Grass	Forb	Litter	Total	Total - Litter	
18	0	1	24	43	19	0.009058099
1	3	1	27	32	5	0.010423257
2	17	0	7	26	19	0.009278486
24	0	14	19	57	38	0.019452383
27	0	0	49	76	27	0.021216075
8	2	0	10	20	10	0.011410407
22	0	1	111	134	23	0.005938089
2	3	5	154	164	10	0.006168341
2	1	2	4	9	5	0.004107299
1	1	1	2	5	3	0.003598496
1	5	1	1	8	7	0.003369051
1	0	7	15	23	8	0.005379119
1	0	1	6	8	2	0.003327917
1	1	9	1	12	11	0.001844679
16	0	15	16	47	31	0.010361896
6	0	8	20	34	14	0.009353981
6	0	6	20	32	12	0.009700746
8	0	12	35	55	20	0.008547655
35	0	0	80	115	35	0.008813524
11	0	4	40	55	15	0.015189377
7	1	1	11	19	8	0.009764435
0	19	0	11	30	19	0.008504406
0	11	0	15	26	11	0.011529978
1	46	1	2	50	48	0.006571117
0	6	0	2	8	6	0.005155168
1	1	1	1	4	3	0.002258037
3	15	1	23	42	19	0.012193352
0	0	0	3	3	0	0.01093019

APPENDIX D

Residuals from SfM Regression Plots

Histogram of Residuals from AGB – Litter ~ SfM Volume

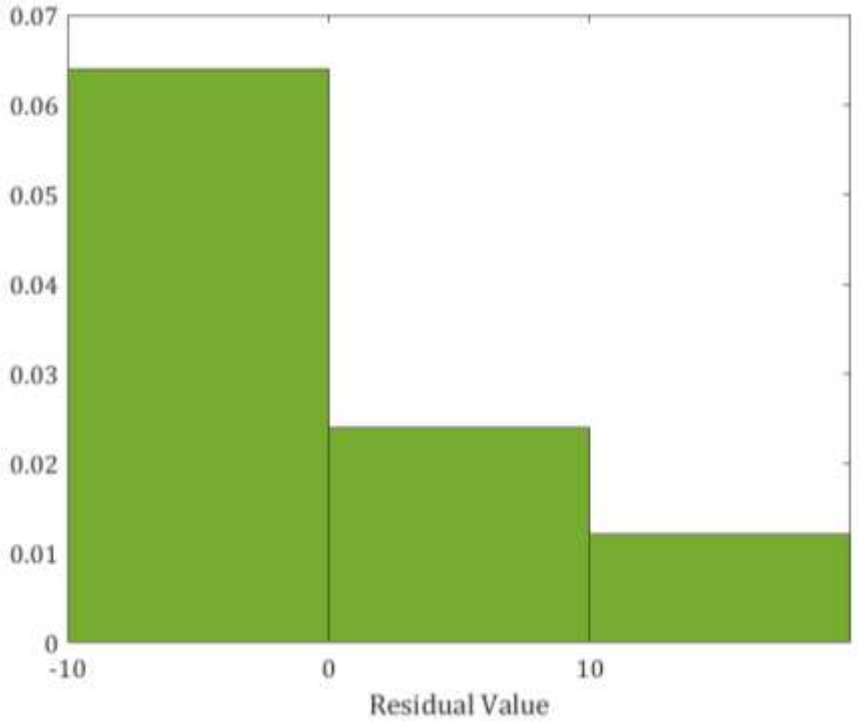

Histogram of Residuals from Linear Regression of ln(AGB – Litter) ~ ln(SfM Volume)